

# Development and Evaluation of a Portable Device for Measuring Curling and Warping in Concrete Pavements

**Final Report**  
**January 2016**



**IOWA STATE UNIVERSITY**  
**Institute for Transportation**

---

## **Sponsored by**

Iowa Department of Transportation  
(Part of InTrans Project 13-486)  
Federal Highway Administration  
Midwest Transportation Center  
U.S. Department of Transportation Office of  
the Assistant Secretary for Research and Technology

## **About MTC**

The Midwest Transportation Center (MTC) is a regional University Transportation Center (UTC) sponsored by the U.S. Department of Transportation Office of the Assistant Secretary for Research and Technology (USDOT/OST-R). The mission of the UTC program is to advance U.S. technology and expertise in the many disciplines comprising transportation through the mechanisms of education, research, and technology transfer at university-based centers of excellence. Iowa State University, through its Institute for Transportation (InTrans), is the MTC lead institution.

## **About InTrans**

The mission of the Institute for Transportation (InTrans) at Iowa State University is to develop and implement innovative methods, materials, and technologies for improving transportation efficiency, safety, reliability, and sustainability while improving the learning environment of students, faculty, and staff in transportation-related fields.

## **ISU Non-Discrimination Statement**

Iowa State University does not discriminate on the basis of race, color, age, ethnicity, religion, national origin, pregnancy, sexual orientation, gender identity, genetic information, sex, marital status, disability, or status as a U.S. veteran. Inquiries regarding non-discrimination policies may be directed to Office of Equal Opportunity, Title IX/ADA Coordinator, and Affirmative Action Officer, 3350 Beardshear Hall, Ames, Iowa 50011, 515-294-7612, email [eooffice@iastate.edu](mailto:eooffice@iastate.edu).

## **Notice**

The contents of this report reflect the views of the authors, who are responsible for the facts and the accuracy of the information presented herein. The opinions, findings and conclusions expressed in this publication are those of the authors and not necessarily those of the sponsors.

This document is disseminated under the sponsorship of the U.S. DOT UTC program in the interest of information exchange. The U.S. Government assumes no liability for the use of the information contained in this document. This report does not constitute a standard, specification, or regulation.

The U.S. Government does not endorse products or manufacturers. If trademarks or manufacturers' names appear in this report, it is only because they are considered essential to the objective of the document.

## **Quality Assurance Statement**

The Federal Highway Administration (FHWA) provides high-quality information to serve Government, industry, and the public in a manner that promotes public understanding. Standards and policies are used to ensure and maximize the quality, objectivity, utility, and integrity of its information. The FHWA periodically reviews quality issues and adjusts its programs and processes to ensure continuous quality improvement.

## **Iowa Department of Transportation Statements**

Federal and state laws prohibit employment and/or public accommodation discrimination on the basis of age, color, creed, disability, gender identity, national origin, pregnancy, race, religion, sex, sexual orientation or veteran's status. If you believe you have been discriminated against, please contact the Iowa Civil Rights Commission at 800-457-4416 or the Iowa Department of Transportation affirmative action officer. If you need accommodations because of a disability to access the Iowa Department of Transportation's services, contact the agency's affirmative action officer at 800-262-0003.

The preparation of this report was financed in part through funds provided by the Iowa Department of Transportation through its "Second Revised Agreement for the Management of Research Conducted by Iowa State University for the Iowa Department of Transportation" and its amendments.

### Technical Report Documentation Page

<b>1. Report No.</b> Part of InTrans Project 13-486	<b>2. Government Accession No.</b>	<b>3. Recipient's Catalog No.</b>	
<b>4. Title and Subtitle</b> Development and Evaluation of a Portable Device for Measuring Curling and Warping in Concrete Pavements		<b>5. Report Date</b> January 2016	
		<b>6. Performing Organization Code</b>	
<b>7. Author(s)</b> Halil Ceylan, Robert F. Steffes, Kasthurirangan Gopalakrishnan, Sunghwan Kim, Shuo Yang, and Kailin Zhuang		<b>8. Performing Organization Report No.</b> Part of InTrans Project 13-486	
<b>9. Performing Organization Name and Address</b> Institute for Transportation Iowa State University 2711 South Loop Drive, Suite 4700 Ames, IA 50010-8664		<b>10. Work Unit No. (TRAIS)</b>	
		<b>11. Contract or Grant No.</b> Part of DTRT13-G-UTC37	
<b>12. Sponsoring Organization Name and Address</b> <div style="display: flex; justify-content: space-between;"> <div style="width: 45%;">           Iowa Department of Transportation            800 Lincoln Way            Ames, IA 50010            Midwest Transportation Center            2711 S. Loop Drive, Suite 4700            Ames, IA 50010-8664         </div> <div style="width: 45%;">           Federal Highway Administration and            U.S. Department of Transportation            Office of the Assistant Secretary for            Research and Technology            1200 New Jersey Avenue, SE            Washington, DC 20590         </div> </div>		<b>13. Type of Report and Period Covered</b> Final Report	
		<b>14. Sponsoring Agency Code</b>	
<b>15. Supplementary Notes</b> Visit <a href="http://www.intrans.iastate.edu">www.intrans.iastate.edu</a> for color pdfs of this and other research reports.			
<b>16. Abstract</b> <p>Portland cement concrete (PCC) pavement undergoes repeated environmental load-related deflection resulting from temperature and moisture variations across pavement depth. This has been recognized as resulting in PCC pavement curling and warping since the mid-1920s. Slab curvature can be further magnified under repeated traffic loads and may ultimately lead to fatigue failures, including top-down and bottom-up transverse, longitudinal, and corner cracking. It is therefore significant to measure the “true” degree of curling and warping in PCC pavements, not only for quality control (QC) and quality assurance (QA) purposes, but also for better understanding of its relationship to long-term pavement performance.</p> <p>Although several approaches and devices—including linear variable differential transducers (LVDTs), digital indicators, and some profilers—have been proposed for measuring curling and warping, their application in the field is subject to cost, inconvenience, and complexity of operation. This research therefore explores developing an economical and simple device for measuring curling and warping in concrete pavements with accuracy comparable to or better than existing methodologies. Technical requirements were identified to establish assessment criteria for development, and field tests were conducted to modify the device to further enhancement. The finalized device is about 12 inches in height and 18 pounds in weight, and its manufacturing cost is just \$320. Detailed development procedures and evaluation results for the new curling and warping measuring device are presented and discussed, with a focus on achieving reliable curling and warping measurements in a cost-effective manner.</p>			
<b>17. Key Words</b> concrete moisture—concrete pavements—concrete temperature—curling and warping—measurement device—portable device		<b>18. Distribution Statement</b> No restrictions.	
<b>19. Security Classification (of this report)</b> Unclassified.	<b>20. Security Classification (of this page)</b> Unclassified.	<b>21. No. of Pages</b> 84	<b>22. Price</b> NA



# **DEVELOPMENT AND EVALUATION OF A PORTABLE DEVICE FOR MEASURING CURLING AND WARPING IN CONCRETE PAVEMENTS**

**Final Report  
January 2016**

## **Principal Investigator**

Halil Ceylan, Professor, Civil, Construction, and Environmental Engineering (CCEE)  
Director, Program for Sustainable Pavement Engineering and Research (PROSPER)  
Institute for Transportation, Iowa State University

## **Co-Principal Investigators**

Robert F. Steffes, Research Engineer  
Kasthurirangan Gopalakrishnan, Research Associate Professor  
Sunghwan Kim, Research Scientist  
Institute for Transportation, Iowa State University

## **Research Assistants**

Shuo Yang and Kailin Zhuang

## **Authors**

Halil Ceylan, Robert F. Steffes, Kasthurirangan Gopalakrishnan, Sunghwan Kim,  
Shuo Yang, and Kailin Zhuang

## **Sponsored by**

Iowa Department of Transportation,  
Federal Highway Administration,  
Midwest Transportation Center, and  
U.S. Department of Transportation  
Office of the Assistant Secretary for Research and Technology

Preparation of this report was financed in part  
through funds provided by the Iowa Department of Transportation  
through its Research Management Agreement with the  
Institute for Transportation  
(Part of InTrans Project 13-486)

## **A report from**

### **Institute for Transportation**

#### **Iowa State University**

2711 South Loop Drive, Suite 4700

Ames, IA 50010-8664

Phone: 515-294-8103 / Fax: 515-294-0467

[www.intrans.iastate.edu](http://www.intrans.iastate.edu)



## TABLE OF CONTENTS

ACKNOWLEDGMENTS .....	ix
EXECUTIVE SUMMARY .....	xi
1. INTRODUCTION .....	1
1.1 Problem Statement .....	1
1.2 Research Objectives and Approaches .....	2
2. LITERATURE REVIEW .....	3
2.1 Curling and Warping .....	3
2.2 Review of the Currently Available Technologies/Devices for Measuring Slab Curling Behaviors .....	5
2.3 Summary of Literature Review Results .....	28
3. DESIGN APPROACH OF THE ISU PORTABLE CURLING AND WARPING MEASUREMENT DEVICE .....	29
3.1 Design Criteria .....	29
3.2 Development of First-Generation Prototype .....	29
3.3 Principle of Operation .....	32
4. DEVICE ENHANCEMENTS AND EVALUATIONS .....	33
4.1 First-Generation Prototype .....	33
4.2 Second-Generation Prototype .....	33
4.3 Third-Generation Prototype .....	39
4.4 Fourth-Generation Prototype .....	49
4.5 Summary of the Developed Prototype of Device .....	52
5. SUMMARY .....	55
REFERENCES .....	57
APPENDIX A. FOURTH-GENERATION ISU CURLING AND WARPING MEASUREMENT DEVICE .....	63
APPENDIX B. FOURTH-GENERATION ISU CURLING AND WARPING MEASUREMENT DEVICE SCHEMATIC .....	65
APPENDIX C. ISU CURLING AND WARPING MEASUREMENT DEVICE OPERATION MANUAL .....	67

## LIST OF FIGURES

Figure 1. Stresses exerted due to curling and warping: tensile stress exerted at top in PCC slab with upward curvature (top) and tensile stress exerted at bottom in PCC slab with downward curvature (bottom) .....	4
Figure 2. LVDT used for vertical deflection measurement .....	6
Figure 3. Digital indicators used for curling and warping measurement .....	7
Figure 4. Rod and level measurement principle .....	8
Figure 5. Laser based rod and level device: rotary laser level (upper left), Smart Rod (upper right), and DigiRod (bottom) .....	10
Figure 6. Straight edge .....	11
Figure 7. Straight edge used for rutting depth measurement .....	11
Figure 8. Gauges: shim gauge (left) and taper gauge (right) .....	12
Figure 9. Typical profilograph operation .....	12
Figure 10. RTRRMs mounted on a passenger vehicle .....	13
Figure 11. Inertial profilers: high-speed profiler (left) and lightweight profiler (right) .....	14
Figure 12. Dipstick profiler .....	15
Figure 13. Walking profilometer .....	16
Figure 14. Merlin: image (left) and basic schematic diagram (right) .....	17
Figure 15. ALPS equipment .....	18
Figure 16. ALPS 2 equipment .....	19
Figure 17. ALPS 2 profile example .....	19
Figure 18. Average rectified slope .....	20
Figure 19. Pavement smoothness index category: HMA pavement (left) and PCC pavement (right) .....	21
Figure 20. LiDAR systems: airborne laser scanner (left), mobile laser scanner (center), and terrestrial laser scanner (right) .....	23
Figure 21. Schematic diagram of ALS .....	24
Figure 22. Schematic diagram of mobile laser scanner .....	25
Figure 23. Theory of using time-of-flight-based LiDAR system .....	26
Figure 24. Curling and warping measurement by using TLS .....	28
Figure 25. First generation of ISU curling and warping device: front view (top left), back view (top right), and side view from head (bottom) .....	30
Figure 26. Triangular measuring gauge .....	31
Figure 27. Improvements made for second generation of ISU curling and warping measurement device: small feet (upper left), anchor (upper right), and additional holes on the flanges of U-groove wheel in column A (bottom) .....	34
Figure 28. Overview of second generation of ISU curling and warping measurement device .....	35
Figure 29. Field test site on ISU campus .....	35
Figure 30. Field test on October 24, 2014: vertical view (left) and horizontal view (right) .....	36
Figure 31. Profile measurements: at the joint (left) and at the center (right) .....	37
Figure 32. Pavement deflection profiles measured on October 24, 2014: profile measured in the morning (left) and profile measured in the afternoon (right) .....	37
Figure 33. Comparison between morning and afternoon measurements on October 24, 2014 .....	38



Figure 34. Accessories (clips and pins) .....	39
Figure 35. Demonstration of using accessories in the laboratory .....	40
Figure 36. Field test on November 10, 2014: setup overview (left) and clips used in the ends (right) .....	41
Figure 37. Diagonal profile measuring on November 10, 2014 .....	41
Figure 38. Pavement deflection profiles measured on November 10, 2014: profile measured in the morning (left) and profile measured in the afternoon (right) .....	42
Figure 39. Diagonal profile measured in the morning of November 10, 2014 .....	42
Figure 40. Comparison between morning and afternoon measurements on November 10, 2014 .....	43
Figure 41. Rulers evaluated in this study .....	44
Figure 42. Comparison of the alternative rulers in the laboratory .....	46
Figure 43. Field test on April 10, 2014: setup overview (left) and pins used underneath the string in the ends (right) .....	46
Figure 44. Comparison of the three rulers in the field .....	47
Figure 45. Comparison between morning and afternoon measurements on April 10, 2015 .....	48
Figure 46. Improvements made for fourth generation of ISU curling and warping measurement device: shorter head of column A (top left), shorter handle of column B (top right), sharp anchor (bottom left), and replaced cord (bottom right) .....	50
Figure 47. Fourth generation of ISU curling and warping measurement device: column A (left) and column B (right) .....	51
Figure 48. Field test on June 20, 2015: setup overview (left) and measuring using rulers (right) .....	51
Figure 49. Comparison between morning and afternoon measurements on June 20, 2015 .....	52
Figure 50. Final version (fourth generation) of ISU curling and warping device with all accessories .....	53
Figure 51. Three-dimensional illustration of ISU curling and warping device .....	54
Figure A.1. Side view of ISU curling and warping measurement device .....	63
Figure A.2. 3D view of device from column A .....	63
Figure A.3. 3D view of device from column B .....	64
Figure B.1. Dimension diagram of ISU curling and warping measurement device .....	65
Figure C.1. Insert anchor of column A into the joint .....	67
Figure C.2. Unpin the bar and unhook the string .....	67
Figure C.3. Pull the string out .....	68
Figure C.4. Hook up the string in column B .....	68
Figure C.5. Lock the U-groove wheel in column A .....	69
Figure C.6. Adjust the handle of column B to further tighten the string .....	69
Figure C.7. Insert the clips .....	70
Figure C.8. Deploy the measuring tape .....	70
Figure C.9. Take measurements using rulers .....	71

## LIST OF TABLES

Table 1. Comparison among different rod and level devices .....	9
Table 2. Comparison among different LiDAR platforms .....	26
Table 3. Research focusing on using LiDAR systems for pavement inspection .....	27
Table 4. Summary of currently available devices for measuring slab curling behaviors (prices available until July 2015) .....	28
Table 5. Comparison of rulers for measuring curling and warping .....	45
Table 6. Cost of ISU curling and warping measurement device .....	53

## **ACKNOWLEDGMENTS**

The authors would like to thank the Midwest Transportation Center (MTC) and the U.S. Department of Transportation Office of the Assistant Secretary for Research and Technology (USDOT/OST-R) for sponsoring this research. The authors would also like to thank the Iowa Department of Transportation (DOT) and Iowa Highway Research Board (IHRB), which used Federal Highway Administration state planning and research funds as part of their funding and provided match funds for this project through a related study that is still in progress.

Special thanks to Bruce D. Erickson and William Halterman with the Iowa State University Chemistry Machine Shop for their guidance and constructive comments for the device design, manufacture, and modifications in this research.



## **EXECUTIVE SUMMARY**

Temperature and moisture variations across the depth of portland cement concrete (PCC) pavements result in unique deflection behavior that has been characterized as pavement curling and warping since the mid-1920. Repeated slab curvature changes due to curling and warping, combined with traffic loading, can accelerate fatigue failures, including top-down and bottom-up transverse, longitudinal, and corner cracking.

Numerous studies have reported premature transverse cracking resulting from slab curling and warping in concrete pavements, like the recent series of cracks observed in an I-80 section near Adair County, Iowa. This is not only a safety issue, but it also costs transportation agencies time and money to implement repair solutions.

It is therefore of paramount importance to measure the actual magnitude of curling and warping taking place in concrete pavements to develop performance measures and critical threshold magnitudes and to gain a better understanding of their relationship to diurnal and seasonal temperature/moisture changes and long-term pavement performance.

Although several approaches and devices have been proposed for measuring curling and warping in in-service concrete pavements, each of them have certain limitations that inhibit their use for routine inspection for quality control (QC) and quality assurance (QA). There is therefore an urgent need to develop an economical and simple device for measuring curling and warping in concrete pavements with accuracy comparable to or better than that of existing methodologies.

This research was directed toward developing and evaluating a self-made Iowa State University (ISU) curling and warping measurement device capable of providing accurate curling and warping measurements in the field. The ISU curling and warping device has been specially designed to be a portable, easy-to-use, reliable, and economical instrument for facilitating a large number of measurements across the state to produce a database correlating curling and warping measurements with concrete performance and other properties.

A first-generation crude prototype of this proposed device had already been developed to support ongoing research efforts at ISU focusing on investigating the impact of curling and warping on concrete pavements.

After several field tests and improvements, the latest version of this device consists of two approximately 12-inch-long hollow steel columns that can position a string above a concrete pavement surface at a predetermined elevation. The string can be tightened by adjusting rollers on the columns so that displacement between the string and pavement surface can be used to represent curling and warping magnitudes.

Device transportation, setup, and measurement operations in the field can be done easily by one adult operator.

The results from field tests have demonstrated fast and accurate measurements with a low instrument cost of \$320. It is anticipated that this proposed device from ISU could be used for standard curling and warping measurements in the field and thus lead to improvement of concrete pavement construction practices.

# **1. INTRODUCTION**

## **1.1 Problem Statement**

Climatic conditions can have significant effects on concrete pavement performance. Moisture and temperature in concrete pavement structures are the two principal environmentally driven variables that can significantly affect pavement layer and subgrade properties and, hence, the load-carrying capacity.

Temperature and moisture variations across the depth of the portland cement concrete (PCC) pavements cause concrete to expand and/or contract at different rates throughout its depth, thereby causing curvature in the slab. Any forces (including self-weight of the slab) that restrain slab curvature induce stresses within the PCC slab (ARA, Inc. 2004). Curvature resulting from temperature variations is referred to as curling, and curvature resulting from moisture variations is referred to as warping. Both the direction (upward or downward) and magnitude of slab curvature varies diurnally and seasonally.

Under repeated slab curvature changes and traffic loading, concrete pavements exhibit fatigue failures, including top-down and bottom-up transverse, longitudinal, and corner cracking (Hiller and Roesler 2005). Recognizing the importance of curling and warping behavior on concrete pavement performance, the new American Association of State Highway and Transportation Officials (AASHTO) Mechanistic-Empirical Pavement Design Guide (MEPDG) and associated software (AASHTOWare Pavement ME Design) considers temperature and moisture effects to predict pavement performance in concrete pavement design (AASHTO 2008, 2013). The recently completed NCHRP 1-47 Project, “Sensitivity Evaluation of MEPDG Performance Prediction,” concluded that slab curling and warping-related properties consistently exhibit the highest sensitivity to concrete pavement performance predictions (Ceylan et al. 2013; Schwartz et al. 2011).

While the impact of curling and warping has been well recognized, there has been no standardized method to measure curling and warping in practice. Various techniques have been explored through previous experimental research studies, including traditional rod and level, installation of strain gages and linear variable differential transformers (LVDTs), digital indicators, and light detection and ranging (LiDAR) technology. These approaches, however, have not proven to be cost effective, take considerable time to install/set up/calibrate, are complex to operate, and produce difficult-to-interpret data. All these limitations inhibit their use for routine inspections for quality control (QC) and quality assurance (QA) of concrete pavements.

There is, therefore, a need for an economical and simple device for measuring curling and warping in concrete pavements with practical accuracy. A user guide developed for such a device could then be used in a standard procedure for routine measurement of curling and warping, leading to improvement of concrete pavement construction practices.

## **1.2 Research Objectives and Approaches**

Curling and warping behavior plays an important role in concrete pavement design (e.g., thickness and joint spacing) and has been drawing attention from transportation agencies since the 1990s (Nantung 2011). Because of a lack of specialized equipment and budget limitations, however, it has been difficult to document the true degree of curling and warping in the field. Existing technologies/devices with potential to measure slab curls have their own limitations, such as high device cost and inconvenience of operation, and they are time and labor consuming. This research, therefore, is directed toward development of a portable, simple, reliable, and economical device to be primarily used for curling and warping measurements in concrete pavements, with accuracy comparable to or better than the existing methodologies. To achieve this goal, currently available technologies/devices with potential to measure concrete slab curling were reviewed and evaluated; their limitations were also identified. This led to establishment of design criteria for the development of a proposed device with promise to be portable, easy to operate by just one person, and capable of providing reliable measurements. Performance of the fabricated device was assessed in field tests and different prototype devices were made, each with enhancements based on learning experiences from field evaluation tests. An operation manual for the developed devices was also produced.

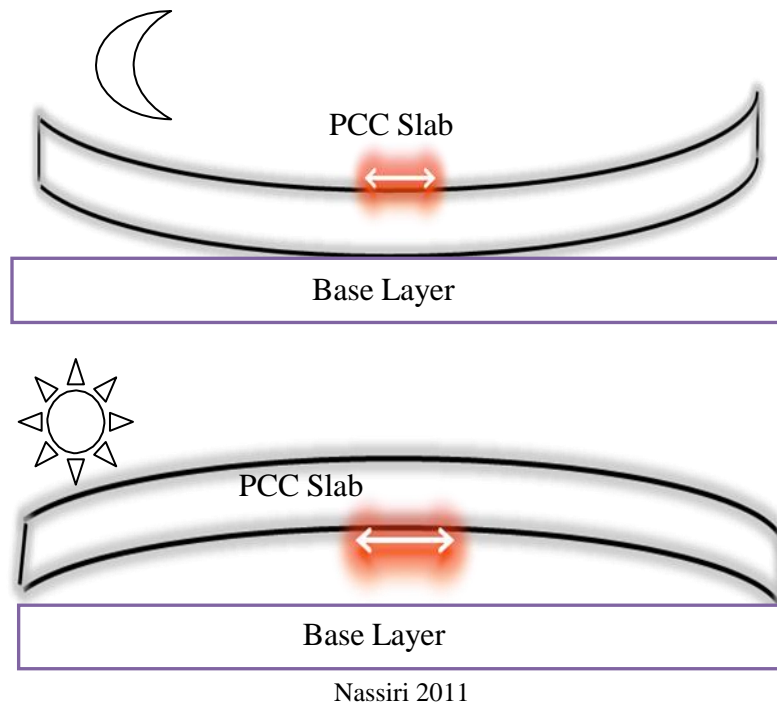


## **2. LITERATURE REVIEW**

### **2.1 Curling and Warping**

Curling and warping of a concrete pavement slab refer to its upward or downward deformation resulting from changes in environmental conditions; they are common phenomena in concrete structures and have been extensively investigated. In general, conventional concrete pavement can undergo repeated deterioration and deformation due to both cyclic traffic load and environmental condition changes. Temperature and moisture are the two most significant environmental factors that can influence volumetric changes in PCC. Usually, when the top of a PCC slab has a higher temperature or moisture content, a positive gradient will be induced and the top part of the PCC slab will expand more than the bottom, resulting in downward slab curling or warping. Conversely, if the bottom of a PCC slab has a higher temperature or moisture content than the top, a negative gradient will occur and the bottom part of the slab will expand more than the top, resulting in upward curling or warping of the slab. Generally, a positive temperature gradient occurs during daytime and a negative temperature gradient occurs during nighttime, while a positive moisture gradient occurs during nighttime and a negative moisture gradient occurs during daytime.

Curling and warping can exert stresses, and when concrete slab curvature is induced by nonuniform temperature or moisture gradients, slab restraints will tend to exert tensile stresses resisting the differential strain response throughout the slab depth. Figure 1 illustrates tensile stresses induced in the slab due to nonuniform temperature and moisture gradients and concrete slab restraints.



Nassiri 2011

**Figure 1. Stresses exerted due to curling and warping: tensile stress exerted at top in PCC slab with upward curvature (top) and tensile stress exerted at bottom in PCC slab with downward curvature (bottom)**

The most common restraints of PCC pavement include self-weight of concrete, dowel bars in pavements, and friction between the PCC slab and the base (Wells 2005). Curling and warping stresses in pavements were first investigated by Westergaard during the 1920s. Early researchers, however, including Westergaard, initially treated the temperature profile to exist as a linear relationship throughout the concrete depth (Harik et al. 1994). In the 1930s, a study by Teller and Sutherland (1935) revealed that temperature was distributed nonlinearly within concrete slabs; this could be attributed to material and geometrical nonlinearities (Teller and Sutherland 1935). In that study, it was also found that measured “stresses arising from restrained temperature warping are equal in importance to those produced by the heaviest legal wheel loads” (Teller and Sutherland 1935). Although it was well known that temperature and moisture is highly nonlinearly distributed along slab depth, the majority of methods used in the 1990s to estimate curling and warping stresses were based on an assumption of linear temperature distribution (Harik et al. 1994).

Theoretically, a PCC pavement slab can curl/warp either up or down. Field observations, however, indicate that PCC slabs of pavement more commonly exhibit upward curvature due to long-term dry shrinkage characteristics (Guo and Marsey 2001; Van Dam 2015). During the service life of pavement, the bottom of the slab remains at almost 100% saturation while the surface remains dry, so that it stays in an upward curved shape. Upon rewetting, it may gain back some downward curvature of shrinkage due to a positive gradient, but it will revert back when the surface water disappears. Therefore, PCC slab curvature changes resulting from daily and seasonal temperature and/or moisture gradient changes, characterized as transient curling and warping, are repeatable and reversible. A PCC slab, however, will most likely curl or warp even

without temperature and/or moisture gradient changes during its service life. This behavior is referred to as permanent curling and warping, and it can occur during the setting time of PCC (Nassiri 2011). The setting time of PCC represents the time when PCC becomes hard (Asbahan 2009). During this period, concrete obtains strength and loses moisture and flowability. If temperature and/or moisture gradients develop inside fresh PCC slabs due to high environmental temperature and drying shrinkage during the curing period prior to final set, upward slab curvature can develop. This permanent and irreversible effect is called built-in curling and warping and it may influence early-age concrete behavior.

As mentioned earlier, nonuniform temperature and moisture-induced curling and warping can exert tensile stress due to slab restraints. Since concrete can sustain much higher compressive stress than tensile stress, tensile stress concerns dominate concrete pavement structural design. Generally a longer, wider, or thinner PCC slab can exhibit high tensile interior stress if temperature and moisture gradients are developed. When such tensile stress exceeds the tensile strength of early-aged concrete, cracking will be initiated; when combined with repetitive vehicle loads, such exerted tensile stress can be further magnified and aggravate such cracking, affecting long-term performance and structural capacity of the pavement. Curling and warping-induced curvature is most noticeable at slab corners and joints and can easily damage joints and create interior voids, thereby causing more severe pavement deterioration (Cement Concrete & Aggregate Australia 2006; Mailvaganam et al. 2000; Suprenant and Malisch 1999). Briefly, the curling and warping will have significant influence on the degree of support offered by the subgrade, the stiffness along the joint, and the pavement smoothness (Armaghani et al. 1986, 1987; Ceylan et al. 2005, 2007). It is therefore necessary to measure and monitor curling and warping during routine inspection of concrete pavements for QC and QA. Such inspection will help in developing design and construction strategies to minimize effects of curling and warping on overall concrete pavement performance.

## **2.2 Review of the Currently Available Technologies/Devices for Measuring Slab Curling Behaviors**

Many current methods for measuring slab curling behaviors are not designed for directly measuring the actual degree of curling and warping in an entire PCC slab. Instead, they measure local displacements of a PCC slab or pavement surface profile and then infer the degree of curling and warping. A review of these methods is given in the following sections.

### ***2.2.1 Linear Variable Differential Transducers (LVDTs)***

The LVDT is a common type of electromechanical transducer that enables measurement of very small displacements of up to a few millionths of an inch (Macro Sensors 2014). It is currently the most common device used in the field to investigate curling and warping behavior (Ceylan et al. 2005; Kim et al. 2010; Lederle et al. 2011; Rao and Roesler 2005). This transducer converts mechanical displacement into a corresponding electrical signal containing both phase (for direction) and amplitude (for distance) information. Its operation relies on electromagnetic coupling rather than electrical contact between the probe and the transformer, making it suitable

for harsh environment application by providing long service life and high reliability. Figure 2 illustrates an LVDT used to measure displacement of local area in a PCC slab.



Lim et al. 2011, MnDOT

**Figure 2. LVDT used for vertical deflection measurement in concrete pavement**

Linear variable differential transformers can provide long-term, continuous, real-time, highly accurate, and reliable displacement measurements. Theoretically, an LVDT can produce infinite resolution by producing outputs corresponding to even infinitesimally small changes in core position. Readability of the external electronic display and noise in an LVDT signal conditioner represents the only limitations of LVDT resolution. Another benefit of LVDTs is that the road closure is not required when LVDTs are embedded inside pavements, but LVDT instrumentation placement must be accomplished prior to paving operations in newly constructed pavement or instrumented through retrofitting slabs for existing pavement. The instrumentation processes are also usually expensive and time consuming. Generally, one LVDT can monitor only a single-direction continuous deflection change (usually up or down deflection) at one fixed position inside the concrete. To obtain comprehensive deflection data for one PCC slab, multiple LVDTs must be installed at least at critical locations (e.g., slab corners, mid-edge, and slab center). The general cost of one LVDT can be approximately \$500 and the accompanying data-logger may cost \$2,000, so it can be an extremely costly method for curling and warping measurements in a long pavement section. Moreover, sensor survivability will be a concern because of the potential for cable damage and corrosion both during construction and during later service life even if the LVDT itself has been originally designed for harsh climatic conditions.

### *2.2.2 Digital Indicators*

A digital indicator is another possible method that can be used to capture curling and warping behavior of concrete pavement (see Figure 3).



Johnson et al. 2010

**Figure 3. Digital indicators used for curling and warping measurement**

It is a type of stationary measuring system capable of detecting tiny elevation changes ranging from 0.0001 inch to 1 inch at a single position. Prior to measurement, digital indicators can be placed along the wheel path of traffic lanes and attached to a base (e.g., a steel bar) placed on the shoulder to restrain their movement, as shown in Figure 3.

During a measurement, these indicators can be suspended over the pavement surface to capture continuous pavement profile changes to be transmitted to a computer for automatic data recording. Advantages of digital indicators, such as continuous and real-time monitoring, are similar to those of LVDTs. Unlike LVDTs, digital indicators need not be installed prior to concrete placement and do not suffer adversely from high alkali environments. This technology, however, requires road closure during measurements and can only be used to investigate built-in curling and warping in the limited period between concrete finishing and traffic opening (Johnson et al. 2010).

### *2.2.3 Rod and Level*

Rod and level is the traditionally most common and simplest method of profiling a segment of roadway surface. This method provides a static measurement of the “true profile” and can thus be used as a reference device for calibrating other profiling devices. As suggested by its name, a rod and level system usually consists of an optical level and a graduated rod. Figure 4 is a schematic diagram showing the operation of a traditional rod and level.

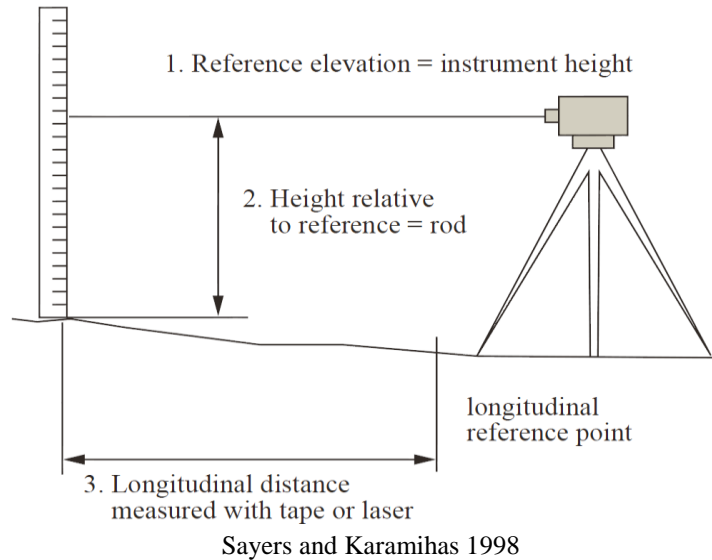


**Figure 4. Rod and level measurement principle**

It can be seen that the surface elevation is obtained by recording the reference elevation and longitudinal distance at constant intervals along a line on a traveled surface. This line, also called a “wheeltrack,” represents the path followed by a vehicle tire. A roughness index can be obtained by inputting longitudinal profile points into a computational algorithm. Standard rod and level operational procedures are specified by ASTM E1364-95 (ASTM 2012a). According to this standard, the interval along a wheeltrack shall not be larger than 1.0 or 2.0 feet, depending on the class of resolution. Measurements by this method require at least two people—one to locate and hold the graduated rod and another to read relative heights and record readings from the leveling instrument. For better efficiency, use of a third person for recording the readings is usually recommended.

The rod and level method offers a simple way of obtaining a standard roughness index using generic equipment (ASTM Standard E1364-95 (ASTM 2012a)). It usually provides relatively sufficient accuracy measurements for laying out a road. Because it was originally designed for true pavement surface profile measurement, it also can be used for curling and warping inspection. Even though this method is simple, however, it is also extremely labor intensive. It requires at least two people to carry the equipment, has a very slow operational speed ( $< 0.006$  mph), and requires road closure during measurement, which is a possible major safety concern (Olson and Chin 2012). Furthermore, the requirements pertaining to the rod and level method for roughness measurements are much more stringent than for normal surveying purposes; it usually requires a resolution of approximately 0.02 in. (0.5 mm), whereas a normal surveying rod usually has a resolution of 0.25 in. (5 mm); resolution of some rulers can be up to 1 mm. Therefore, more accurate readings must rely on a micrometer within the optical level to achieve a resolution of about 0.1 mm. For example, during pavement profile measurement, 10 mm values are obtained visually from the rod and 0.1 mm values can be obtained from the micrometer to interpolate between marks on the rod. The profile obtained can be accurate to 0.1 mm and can be used to calibrate response-type measuring systems.

A digital ruler can be used to speed up measurements, and the longitudinal distance, typically measured by a tape, can be replaced by a laser-based system. Automated techniques can be useful for curling and warping measurements over relatively large areas to improve operational speed. Nevertheless, automated techniques will induce extra cost. Laser-system-based rod and level as well as rotary laser level, Smart Rod, and DigiRod are listed and compared in Table 1.

**Table 1. Comparison among different rod and level devices**

<b>Type</b>	<b>Accuracy</b>	<b>Max Distance</b>	<b>Price</b>
Rod and level	1/4 in.	200 ft	\$240~\$350
Rotary laser level	1/4 in.	800 ft	\$500~\$700
Smart Rod	3/32 in.	N/A	\$535
DigiRod	1/16 in.	160 ft	\$620

Figure 5 shows electronic rod and level systems.





CST/berger no date upper left, AGL Laser 2010 upper right, Trimble Inc. 2015 bottom

**Figure 5. Laser based rod and level device: rotary laser level (upper left), Smart Rod (upper right), and DigiRod (bottom)**

#### 2.2.4 Straight Edge

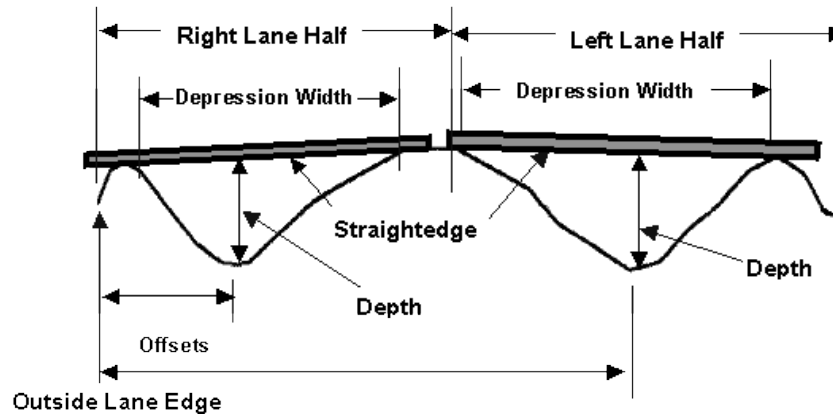
In addition to rod and level, straight edge is also a simple and widely used method for inspecting surface irregularities in road construction, particularly for rut-depth measurement on flexible pavement. Because it measures downward displacement of pavements, it can be used for measuring curling and warping. A straight edge is usually comprised of a relatively large aluminum beam of a certain length along with a measuring gauge. Figure 6 and Figure 7 illustrate a general straight-edge device and a schematic diagram for depth measurement.





MATEST

**Figure 6. Straight edge**

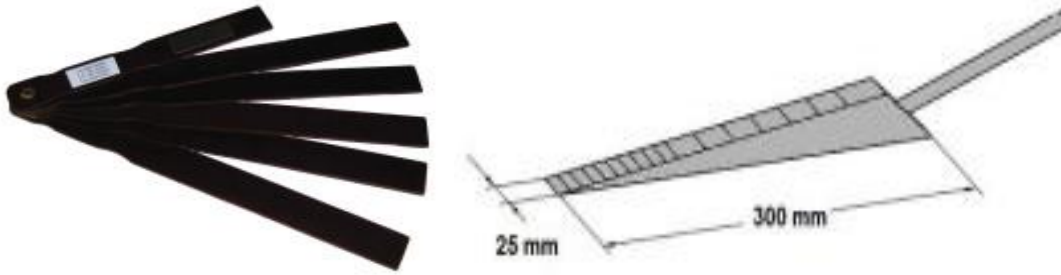


Elkins et al. 2003, FHWA

**Figure 7. Straight edge used for rutting depth measurement**

Standard test procedures that specify a standard aluminum beam length in the range of 5.67 feet to 16 feet are described in ASTM E1703-10 (2010). During the measurement, a gauge is used to determine depth. The gauge shall be capable of measuring a distance of at least 0.75 in. (19 mm) with an accuracy of at least 1/16 in. or 1 mm.

A straight edge can be used to assess smoothness for both flexible pavement and rigid pavement, as specified in *Standards for Specifying Construction of Airports* (FAA 2009). The typical price of a straight edge for pavement inspection can vary from \$150 to \$2,000, depending on length of the beam. For measurement convenience, a shim gauge and a taper gauge can be used to measure the gap between the aluminum beam and the pavement surface, as shown in Figure 8.



Mike Petsch & Associates, Inc. no date

**Figure 8. Gauges: shim gauge (left) and taper gauge (right)**

Use of such gauges enables rapid field measurement with resolutions of 1/16 in. and 1 mm, respectively. A shim gauge costs \$80, and a taper gauge costs \$280.

The straight-edge method has potential for easy and fast measurement of curling and warping on concrete slabs, but its main disadvantages are the fixed length and relative heavy weight of the aluminum beam. Furthermore, depth values obtained using a straight-edge measuring method may not correlate well with values obtained using other methods (ASTM Standard E1703-10 2010).

### 2.2.5 Profilographs

A profilograph, usually used for roughness measurement (e.g., profile index) on newly constructed pavements, is a truss-type device consisting of a metal frame equipped with several supporting single-axle wheels. Figure 9 shows a typical profilograph that looks like a rolling straight edge.



Wright-Kehner 2015, © 2015 Arkansas State Highway and Transportation Department (AHTD)

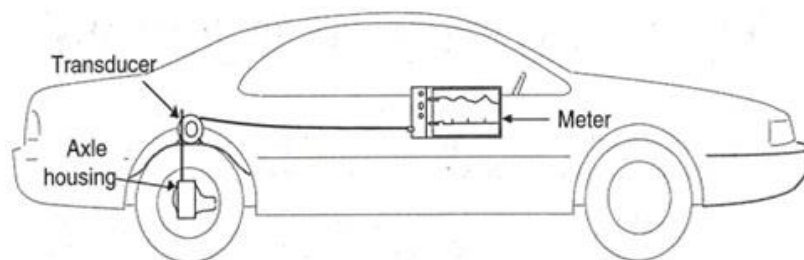
**Figure 9. Typical profilograph operation**

Generally, the length of a profilograph can be up to 33 feet, with a 25-foot-long truss and 4 to 12 supporting wheels (Olson and Chin 2012). In addition to the supporting wheels, a profile wheel is mounted at the bottom center to allow for free vertical motion. This wheel is connected to a recorder so that its vertical motion can be recorded. During a measurement, the motion of the profile wheel and its deviation from a reference plane established from the other wheels on this rigid frame will be automatically recorded on a paper strip chart with a scale of 25 feet/inch in the horizontal direction (Olson and Chin 2012). A profilograph is usually capable of capturing very slight surface undulations up to approximately 20 feet long, and it requires only one or two people to perform assembly and measurement (Pavement Interactive 2010). Its vertical motion measurements can be accurate within at least 0.01 inches.

Profilographs have various forms involving different configurations of wheels and operational procedures (Pavement Interactive 2007). The most common profilograph used by State Highway Administrations (SHAs) is the California profilograph. A common limitation of profilographs is their relatively slow measuring speed, just 2 or 3 mph and slower-than-normal walking speed. Furthermore, a profilograph usually has a limited wavelength, and this may result in a poor measurement and create a biased profile (Olson and Chin 2012). It may amplify and attenuate the true pavement surface profile, raising concerns about the suitability of using this device for smoothness assessment (Perera et al. 2005). It is also hard to correlate its output to magnitudes of curling and warping. The general estimated cost of a profilograph is approximately \$8,000.

#### *2.2.6 Response Type Road Roughness Meters (RTRMs)*

Response type road roughness meters (RTRMs, sometimes also called “road meters”) are designed to measure vehicle bounce response caused by pavement roughness. The meter is mounted either between the rear axles on the frame of a passenger vehicle or on an axle of a trailer relative to the vehicle frame. It is usually also equipped with a displacement transducer mounted on the axle or the trailer to detect tiny increments of axle movement with respect to the vehicle frame during driving. The vehicle can travel at a speed of 50 mph (80 km/hr), and increments of 0.125 inch can be measured. This type of meter was developed in the 1970s and is still used by many countries today. They are comparatively inexpensive, easy to use, and relatively accurate with careful calibration (Janoff and Hayhoe 1990). Figure 10 illustrates a typical RTRM installed on a small vehicle.



FHWA 2002

**Figure 10. RTRMs mounted on a passenger vehicle**

Although RTRRMs are efficient for long pavement measurements, they still have limitations, including calibration issues. They require frequent calibration because of variations in vehicle type, road meter type, driving speed, and wind effects. Furthermore, results tend to vary from one system to another and sometimes turn out to be inconsistent with time; it is also hard to correlate the results to actual curling and warping magnitude. A whole system of RTRRMs usually costs between \$8,000 and \$10,000, depending on manufacturer (University of Utah Civil Engineering Students Creative Commons 2011). ASTM E1082 and E1215 specify the requirements for equipment and operational procedures of RTRRMs (ASTM 2012b, 2012c).

### *2.2.7 High Speed Profilers*

As the name implies, high-speed profilers are designed for reliable pavement profile measurement and computation at highway speed (approximately 70 mph). The most common type of such profilers is the high-speed inertial profiler most often used for in-service pavement inspection. Low-speed and lightweight inertial profilers also exist. This latter type of profiler is relatively small and must be operated at a low speed (from 5 to 30 mph) and its use therefore often requires road closure. Unlike high-speed profilers, lightweight profilers are primarily used for newly constructed PCC pavement before traffic opening because the pavement may not be strong enough to support a relatively heavy vehicle (e.g., a van or a truck) during assessment. Figure 11 shows high-speed and lightweight inertial profilers.



Ames Engineering 2015

**Figure 11. Inertial profilers: high-speed profiler (left) and lightweight profiler (right)**

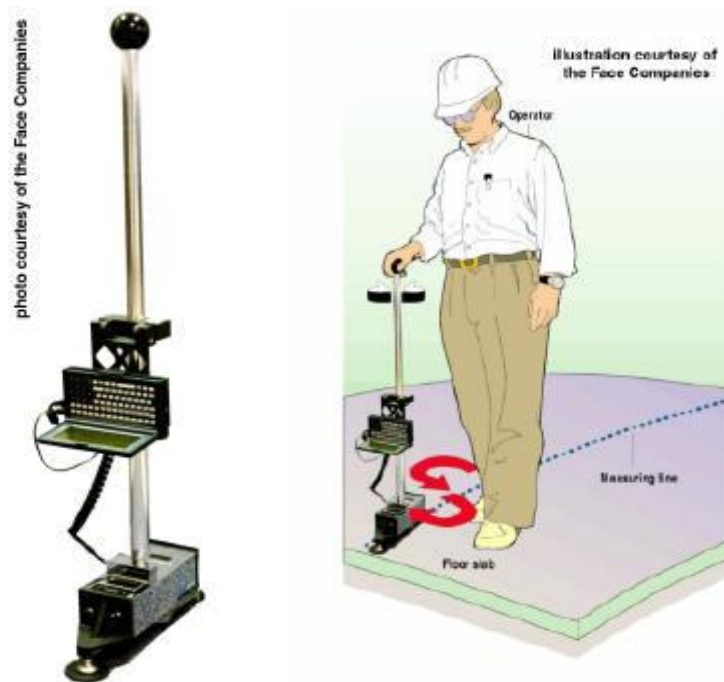
A high-speed inertial profiler is a standard means for measuring large-scale highway pavement (Byrum 2001). Its main components include a height sensor, an accelerometer, a speed/distance measuring system, and an associated computer system. The basic idea underlying the inertial profiler is to correct the height from pavement surface to vehicle measured by a reference height sensor through detection of acceleration responses in the vertical direction during driving. The accelerometer, a transducer usually used to measure vertical acceleration, would be installed at the top of the height sensor to create an inertial reference for measuring vehicle-body motion. Vertical vehicle body motion will then be expressed as vertical displacement mathematically calculated from vertical acceleration. The speed/distance measuring system will also keep tracking the driving distance from the start point.

Height sensors used in high-speed inertial profilers can be generally classified as laser sensors, optical sensors, infrared sensors, or ultrasonic sensors. Among these sensor types, laser sensors mounted at the front of the measuring vehicle are most widely used by SHAs to record longitudinal pavement profile. If multilaser sensors are used, the high-speed inertial profiler can also provide a transverse profile with resolution of up to 0.001 inch. Furthermore, depending on the type of laser sensors, the way they are mounted, and the computer algorithms used, it might be possible to measure grades, cross slope, pavement texture, and pavement distress. General operational procedures for an inertial profiler are given in ASTM E950-09 (ASTM 2009); cost ranges approximately from \$50,000 to \$220,000, depending on manufacturers (University of Utah Civil Engineering Students Creative Commons 2011). Additionally, because these devices use accelerometers, the results will not be sufficiently accurate when the driving speed is less than 10 mph (Sayers and Karamihas 1998).

### 2.2.8 Low-Speed Profilers

#### Dipstick

An inclinometer is a typical handheld profiler commonly used to provide a relatively small-size pavement profile and to calibrate other roughness measurement systems. It is a form of contact-type profiler so the effect on profile measurement from pavement surface texture is minimized (Gerardi et al. 2007). A typical inclinometer profiler, called a “dipstick” (see Figure 12), contains an inclinometer enclosed in a case supported by two feet separated by a 12-inch horizontal distance.



The Face Companies

**Figure 12. Dipstick profiler**



A transverse elevation at one-foot intervals across two lanes of traffic can therefore be measured in one pass. Additionally, two liquid-crystal display (LCD) panels are mounted in each end of the device. The sensor is mounted in such a way that its axis and a line passing through footpad contact points are coplanar (Perera et al. 2002). During measurement, the operator will maneuver the dipstick to walk down a predetermined pavement section by alternately pivoting the dipstick around each foot. During this movement, the sensor will lose balance as the device is pivoted from one foot to the other and the LCD display will become blank (Perera et al. 2002). Each display will show elevation of the feet when its sensor achieves equilibrium and the difference in elevation between the two feet can be recorded.

The dipstick is commonly used to calibrate other complex devices because of its high accuracy (up to 0.005 in. [0.127 mm]), and it also has potential for curling and warping measurements. During measurement, two operators are preferred—one to operate the device and one to record data. A principal advantage of a typical dipstick device is that it does not require complex calibration or highly trained people for operation. This device also has a relatively rapid measuring speed of 10 to 15 measurements per minute compared to that of the traditional rod and level. The dipstick, however, may miss features measured by another profiler because of footpad spacing, and the feature measured may be underestimated compared to that measured by another device because of the long sampling interval. A theoretical analysis by Perera and Kohn (2005) indicated that the long sampling interval of the device may result in measurement contamination due to aliasing if the wavelength corresponds to half that of the normal sampling interval of a dipstick (Perera and Kohn 2005). It also has a much higher initial cost—approximately \$4,500—compared to other traditional methods.

### Walking Profilometer

Similar to inclinometers, a “walking” profilometer (see Figure 13) is also a kind of handheld profiler widely used to quantify pavement roughness; it also has potential for curling and warping measurement.



Morrow 2006

**Figure 13. Walking profilometer**

A “walking” profilometer measures the pavement surface profile using diamond styli, optical sensors, or accelerometers. The roughness is recorded when the device is pushed by the operator at “walking speed,” so these kinds of profilometers and inclinometers are sometimes called “walking profilers.” Unlike inclinometers, the whole system of a typical walking profilometer, including “walking” and data processing, can be automatically controlled by a computer, so it is relatively more effective and faster, with a measuring speed of approximately 3 mph. Its step length (data sample interval) varies among the different devices, and the static resolution of vertical displacement can be as small as 0.0001 in. (0.001 mm) (Morrow 2006). Although a walking profilometer is simple to operate, however, it is subject to adverse effects from the surrounding environment (Morrow 2006). It is also much more expensive than an inclinometer, and its price—depending on manufacturer, type, functions, and model—may be as much as \$30,000.

#### Machine for Evaluating Roughness Using Low-Cost Instrumentation (Merlin)

In addition to the inclinometer and the walking profilometer, another low-speed profiler, the “Merlin” (machine for evaluating roughness using low-cost instrumentation) can be used as a reference device for calibrating other roughness measurement systems such as vehicle mounted bump integrators. The Merlin is an easy-to-use, self-calibrating, robust, and easily maintained profiler with a much lower price than other instruments, typically around \$200 to \$1,000, depending on the country of use. Figure 14 shows an image and a schematic diagram of the Merlin.



Morrow 2006 (left) and Cundill 1991 (right)

**Figure 14. Merlin: image (left) and basic schematic diagram (right)**

Typically, a Merlin consists of a bicycle tire at the front of the main frame, a probe at the middle, and a rear foot and pointer at the rear. The probe records mid-chord deflection and the pointer is used when plotting points onto graph paper (Morrow 2006). Roughness is recorded at regular intervals when the instrument is pushed forward at walking speed. Although the instrument is easy to operate, however, its large size (more than 1.8 m) affects its portability. Moreover, the Merlin does not actually measure the absolute profile but records mid-chord deviations over a predetermined base length along the pavement and then uses a correlation technique to directly

relate statistics from the frequency of those deviations to a smoothness index. It is therefore not suitable for direct curling and warping measurement in the field (Cundill 1991).

### Automated Laser Profile System (ALPS)

Laser-based devices have already proven to be effective tools for pavement profiling. An automated laser profile system (ALPS) developed by the Minnesota Road Research Project (MnROAD) in 2003 is a mobile low-speed profiling device producing highly accurate pavement roughness measurements using laser technology. Figure 15 shows a side view of this mobile profiler.



Worel et al. 2004, MnDOT

**Figure 15. ALPS equipment**

The ALPS was initially designed to measure rut depth in the wheel path. It performs depth measurement using a 14-foot-long ALPS aluminum beam equipped with a high-precision distance measurement laser mounted on its carriage (Worel et al. 2004). The beam is mounted on a lawn tractor that can travel at a speed of 5 to 13 mph. The beam, however, must remain stationary during the measurement. During measurement, distance can be recorded every 0.25 inch and data can be collected over a length of 12 feet and 10 inches (MnDOT 2011).

The ALPS produces reliable results in rutting measurements with a resolution up to 0.0001 inch, more than sufficient for curling and warping measurement. Through further improvements conducted by MnROAD, the ALPS 2 has been developed and designed to analyze curling and warping of concrete pavement, as shown in Figure 16.

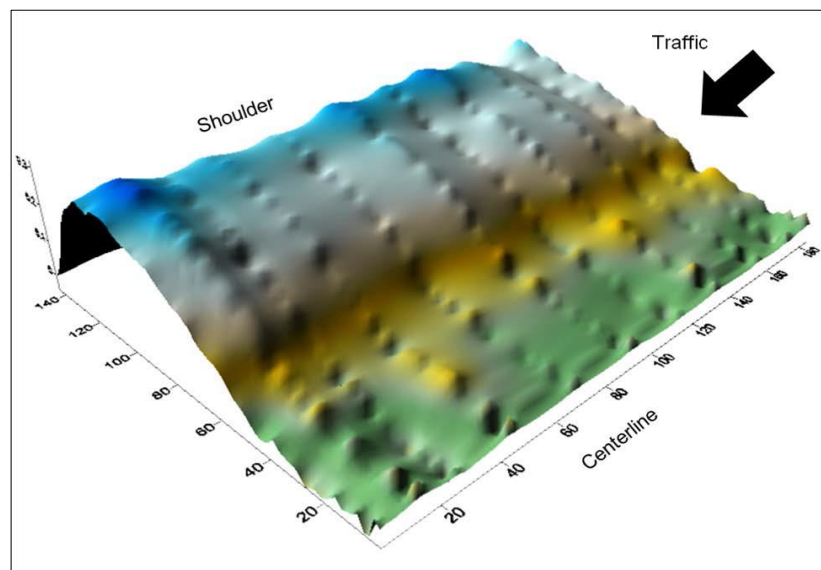




Akkari and Izevbekhai 2012, MnDOT

**Figure 16. ALPS 2 equipment**

The ALPS 2 uses a 15-foot-long beam equipped with laser sensors. The profile is measured at 1-inch intervals in both longitudinal and transverse directions. The output from the ALPS 2 is a three-dimensional (3D) data set (e.g., reading in X, Y, and Z directions) represented as an EXCEL comma-delimited file. The data can be further processed using a sorting macro and then graphed for 3D visualization. Figure 17 is a profile graph from a typical PCC slab.



Akkari and Izevbekhai 2012, MnDOT

**Figure 17. ALPS 2 profile example**

The cost of the ALPS is about \$10,000 not including the lawn tractor and the software.

Profilographs, RTRRMs, low-speed profilers, and high-speed profilers are primarily used for pavement roughness and smoothness measurement. Pavement roughness can be defined as the

deviations of a surface from a true planar surface with characteristic dimensions (see ASTM Standard E867-06 2012d). It represents the irregularities of pavement surface, whereas smoothness represents lack of roughness. Roughness is a significant pavement characteristic for assessment of road quality, and it can be expressed using an international roughness index (IRI) and a profile index (PI). Both these parameters are mathematically determined from a pavement profile collected in the field. Even though curling and warping can be correlated to pavement profile, these devices are not specially designed for curling and warping measurement, and some correlations and modifications may be needed to extend their application for that purpose.

### International Roughness Index (IRI)

The IRI, established in the 1980s, is the most popular worldwide roughness index. It was derived from the International Road Roughness Experiment sponsored by the World Bank in Brazil in 1982 and was subsequently adopted by the Federal Highway Administration (FHWA) as a standard parameter for roughness measurement (FHWA 2005; Huang 2004). The IRI can be represented as a scale of pavement roughness related to a simulated response from a standard vehicle to the roughness induced by a true pavement profile. It is a mathematical transform of a true profile that relates a measured profile to a standard model; the measured profile is usually presented as a summary of the longitudinal surface profile along the wheelpath (Huang 2004). Generally, the IRI can be calculated according to the average rectified slope (ARS), a filtered ratio of a standard vehicle's accumulated suspension motion divided by the distance traveled by the vehicle during the measurement at a standard speed (e.g., 50 mph), as shown in Figure 18.

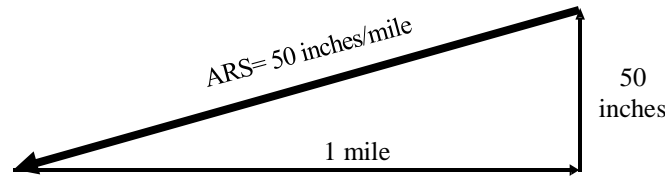


**Figure 18. Average rectified slope**

Therefore, the ARS can be expressed in units of inches per mile or meters per kilometer, and the IRI can be calculated by multiplying the ARS by 1,000, as shown in Equation 1:

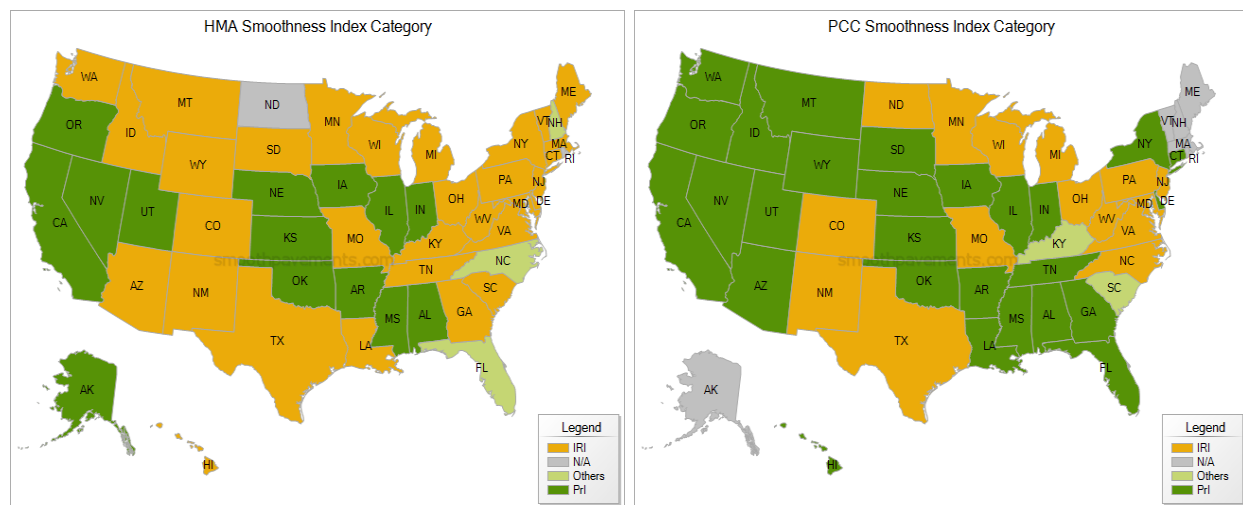
$$IRI = ARS \times 1,000 \text{ (m/km, in./mile)} \quad (1)$$

Because the IRI is usually measured using a moving vehicle (e.g., a profiler), a standard means of calibrating a response-type road-roughness measuring vehicle can be established. ASTM E1170-97 (ASTM 2012e)—“Standard Practices for Simulating Vehicular Response to Longitudinal Profiles of a Vehicular Traveled Surface”—specifies general methods for obtaining vehicle response using simulation of a standard vehicle model. The vehicular response (e.g., vehicle body acceleration) to traveled pavement surface roughness can be calculated for the algorithm developed. In this way, the true IRI can be obtained by processing the measured profile using an algorithm that simulates response of a standard vehicle to a surface profile. The calculated value can then be used as an assessment method for pavement smoothness.

## Profile Index (PI)

The PI is an index defined as the square root of the mean square of profile height in the specified frequency band (Huang 2004). Similar to the IRI, the PI is mathematically determined from a measured surface profile. It can be calculated by counting the number of bumps and dips in the profile trace that fall outside of a blanking band, usually adopted by most highway agencies as 0.2 in. (5 mm) and 0 in. (0 mm) (SmoothPavement 2012). The operational device used for PI measurement is the profilograph, a device that emerged among highway agencies between the 1960s and the 1980s as a popular measuring and controlling device for measuring initial smoothness using profile traces. A profilograph generally has a 25 ft (7.6 m) reference plane capable of producing profile traces (Smith et al. 2002). In such a profile, severe bumps and dips, particularly in PCC pavement, can be identified.

Currently, both the PI and/or the IRI have been selected by the majority of highway agencies as smoothness and roughness specifications for flexible and rigid pavement assessment. Many SHAs measure the pavement profile to calculate the PI and assess smoothness for construction acceptance, and subsequently they use the IRI for pavement performance monitoring. The IRI, however, has increasingly been adopted by SHAs to assess construction acceptance because of technical limitations of profilograph equipment and PI computation procedures as well as the concerns about profilograph accuracy. SHAs still using the PI to check construction acceptance are looking into the possibility of using the IRI for smoothness (Perera et al. 2005; Smith et al. 2002). Figure 19. illustrates the general distribution of states using the IRI and PI on hot mix asphalt (HMA) and PCC pavement for smoothness assessment in the United States.



Transtec Group, Inc. 2012

**Figure 19. Pavement smoothness index category: HMA pavement (left) and PCC pavement (right)**

## Correlation to Curling and Warping

In terms of rough definitions, the PI is used to characterize bumps and dips whereas the IRI is

used to correct localized roughness. Both indices are calculated based on measured pavement surface profiles, and each thus has potential to be converted to the other. Relationships between the IRI and the PI have been proposed by Smith et al. (2002) for asphalt concrete pavement and PCC pavement, respectively. In their study, it was found that pavement type and climatic conditions (e.g., dry-freeze, wet-nonfreeze) are significant factors affecting the relationships between the IRI and the PI (Smith et al. 2002). Another study to investigate the effect of curling and warping on pavement roughness (e.g., IRI) was performed by Karamihas and Senn (2012). That study correlated the relationship between the IRI and curling and warping by using algorithms to estimate pseudo strain gradient (PSG) value—i.e., the gross strain gradient required to deform PCC slabs into the shape present in the measured road profile (Karamihas and Senn 2012).

Algorithms proposed by Chang et al. (2010) used curve fitting between the Westergaard equations-estimated curled/warped PCC slab shape and the measured slab profile to obtain the PSG value (Chang et al. 2010). As a result, the level of curling and warping can be quantified by using the slope of the IRI-PSG relationship to estimate the portion of the IRI associated with curling and warping. It is very hard, however, to directly convert either the IRI or the PI into a true degree of curling and warping, and it is also very difficult to identify locations where such degrees of curling and warping occur, especially using devices that cannot measure a true pavement profile. It is therefore customary to assume that the approaches such as rod and level, straight edge, walking profilers, and inertial profilers have potential for curling and warping measurement because they measure the true road profile. Response type road roughness meters or Merlin, however, cannot be used for curling and warping measurement because they measure the response from the road on the device.

### *2.2.9 Light Detection and Ranging (LiDAR) System*

Light detection and ranging is an active optical remote-sensing technology that measures the properties of pulsed laser beams reflected from an object to acquire relevant information such as x, y, and z coordinates, range, and direction (FDOT 2012). It is currently the most significant geospatial data acquisition technology. Its extreme intensive point cloud data set enables 3D visualization of a scanned area or object, so it is widely used as a surveying tool for topographic inspection and geomaterial mapping (e.g., flood insurance rate mapping, forest and tree mapping, and coastal change mapping). In addition to these conventional applications, the current use of LiDAR has also been extended to transportation infrastructure design and management such as airport obstruction surveying, site characterization, traffic flow estimation, and highway design.

Compared to conventional topographic surveying methods, LiDAR offers competitive advantages of scanning large areas in a very short time, high accuracy (up to 0.001 inch), and incredibly dense collections of data points. It can emit hundreds of thousands of laser beams in just 1 second and determine associated x, y, z coordinates from their reflections. The point cloud made up from the coordinates and associated intensity values from each laser can then be obtained. In this way, a 3D map consisting of hundreds of thousands of data points can be created. Light detection and ranging is sometimes described as a 3D laser scanner. Because of its capability for producing accurate and directly georeferenced spatial information describing

surface characteristics of a scanned object, LiDAR-based platforms have vast potential to be used in characterizing both longitudinal and transverse pavement profiles and pavement surface conditions. Figure 20 shows three common LiDAR platforms: an airborne laser scanner (ALS), a mobile laser scanner (MLS), and a terrestrial laser scanner (TLS).



Olson and Chin 2012

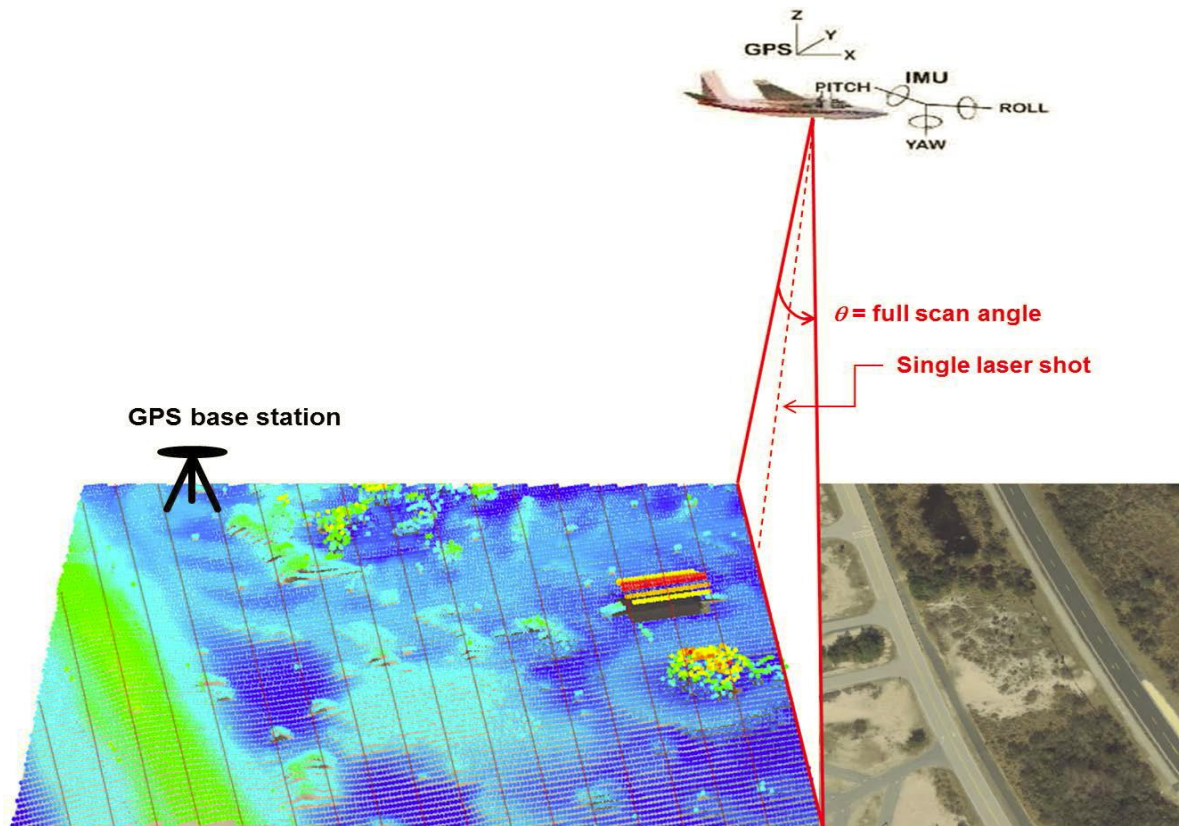
**Figure 20. LiDAR systems: airborne laser scanner (left), mobile laser scanner (center), and terrestrial laser scanner (right)**

#### Airborne Laser Scanner (ALS)

An ALS is a LiDAR system mounted inside a helicopter or an airplane to obtain digital elevation for a target area. It is currently the most effective and efficient tool of topographic mapping for relatively large areas, e.g., approximately 500 million square feet in just 1 hour (Carter et al. 2012). In addition to augmenting traditional topographic mapping to obtain earth elevations, an ALS is also ideal for bathymetric data collection that can be used to map shoreline and near-shore areas. Because of its larger scanning area and its shorter scanning time, an ALS provides the lowest unit cost of operation compared to other platforms.

An ALS measurement is performed when the aircraft is flying, so to calibrate the data bias induced by aircraft motion, an ALS usually collaborates with global positioning (GPS) and inertial measurement unit (IMU) systems mounted inside an aircraft as well. These systems can record position and orientation data of the aircraft so an improved database with accurate location information can be established (Olson and Chin 2012). Figure 21 is a schematic diagram of typical ALS scanning.





NOAA Coastal Services Center

**Figure 21. Schematic diagram of ALS**

It can be seen that an ALS is equipped with a GPS component that can ascertain the x, y, and z coordinates of the LiDAR system to be calibrated by the attendant GPS base station and an IMU system that can provide the accurate attitude of the device. Whereas an ALS is efficient for data collection, however, the data obtained from an ALS may not be accurate and dense enough for curling and warping measurement because of the aircraft altitude and speed. The maximum vertical resolution of commercial airborne LiDAR systems is presently about 2 inches.

### Mobile Laser Scanner (MLS)

Similar to an ALS, an MLS mounts a LiDAR system on a moving vehicle or boat to acquire high-resolution 3D topographic data in the target area while driving. As an emerging flexible technology, an MLS combines global navigation satellite systems (GNSSs) and other sensors such as an IMU and precise odometers to produce highly accurate and precise geospatial data from a moving vehicle (Caltrans 2011). Compared to an ALS, even though an MLS usually has a relatively smaller scanning area and slower moving speed, it offers better accuracy (up to 0.05 inch) and a denser database. It also provides ease of mobilization and lower initial cost.

Figure 22 is a schematic diagram of a typical MLS during measurement.

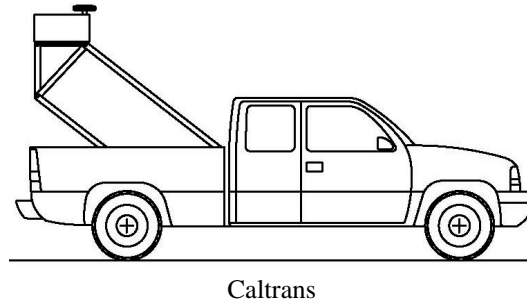


**Figure 22. Schematic diagram of mobile laser scanner**

It can be seen that the laser scanning system is mounted at a high position in the back of the vehicle, unlike previously described inertial profilers that mounted the laser system at a lower position at the front of the vehicle. During MLS scanning, a 2D profile model is first developed, followed by generation of 3D points in collaboration with a GNSS and an IMU. A precise odometer can be used to further improve positioning system accuracy. Additionally, the driving speed and density of point clouds are correlated with the moving speed of an MLS platform that can be varied from 20 to 75 mph. Since lower speed is assumed to provide denser point clouds, traveling speed will vary with the purpose of the application and its accuracy and precision requirements.

An MLS has the potential to be an ideal tool for obtaining an entire surface profile for long stretches of pavement. Current research using MLS for transportation infrastructure, however, has mainly focused on pavement grade and crack identification. There will most likely eventually be a high potential to use an MLS for pavement inspection to produce an IRI and degree of curling and warping. Furthermore, development of a universally accepted standard for device requirements, operational procedures, data processing, and calibration should be addressed.

#### Terrestrial Laser Scanner (TLS)

A TLS is a type of stationary LiDAR system that mounts a rotary laser device on a support tripod (see Figure 20 right). Basically, depending on distance measurement methods, a TLS can be classified into “time-of-flight,” “phase,” or “waveform-processing” based systems, although their fundamental principles are similar in that they use speed of laser beam and time of travel to determine distances from the object to the laser scanner (Caltrans 2011). A time-of-flight-based LiDAR is the most common type of scanner available in the market; a schematic diagram of such a system is given in Figure 23.

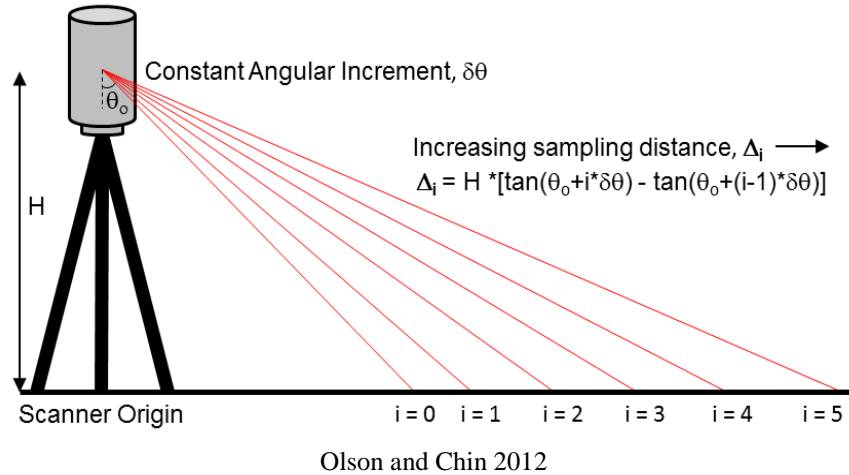


**Figure 23. Theory of using time-of-flight-based LiDAR system**

From this figure it can be seen that laser beams are pulsed from the scanner and deflected at different angles through a rotating mirror. Because the speed of the laser beam is already known, distance can be simply determined by measuring the returning time of pulsed beams. A time-of-flight-based LiDAR system can commonly provide 50,000 points per second (pts) with a working range from 125 to 1,000 m. A phase-based LiDAR system emits a laser beam with multiple phases with sinusoidally modulated optical power. Phase shift will be induced due to reflection from the object, and the change in phase shifts of the returned beam can be determined to calculate the distance according to the unique properties of each individual phase. A phase-based LiDAR has a shorter working range, from 25 to 75 m, but a higher data collection rate. Waveform-processing-based LiDAR, sometimes called “echo digitization,” combines time-of-flight and internal real-time waveform-processing technology to capture the reflected beams. Waveform-processing-based LiDAR usually has a working range similar to time-of-flight-based LiDAR but has a much higher scan rate, up to 300,000 pts (Caltrans 2011, FDOT 2012).

A TLS is the LiDAR platform most investigated by researchers for pavement inspection applications like the IRI, surface texture, cross slope, and crack detection. Compared to an ALS and MLS, a TLS is a type of stationary scanning method that usually provides a smaller scanning range but with higher accuracy (0.001 inch); it therefore has more potential to describe the “true profile” of a pavement surface. Table 2 summarizes the main differences among the common products of three LiDAR platforms.

**Table 2. Comparison among different LiDAR platforms**

Device	Scan Rate (pts)	Cost	Range	Resolution	Potential for Pavement Inspection
ALS	20,000–550,000	\$800,000–\$1,200,000	3–5,800 m	10–150 mm	Low
MLS	30,000–1,000,000	\$600,000	1.5–2,050 m	5–10 mm	Medium
TLS	25,000–1,000,000	\$60,000–\$100,000	1–1,400 m	0.1–1 mm	High



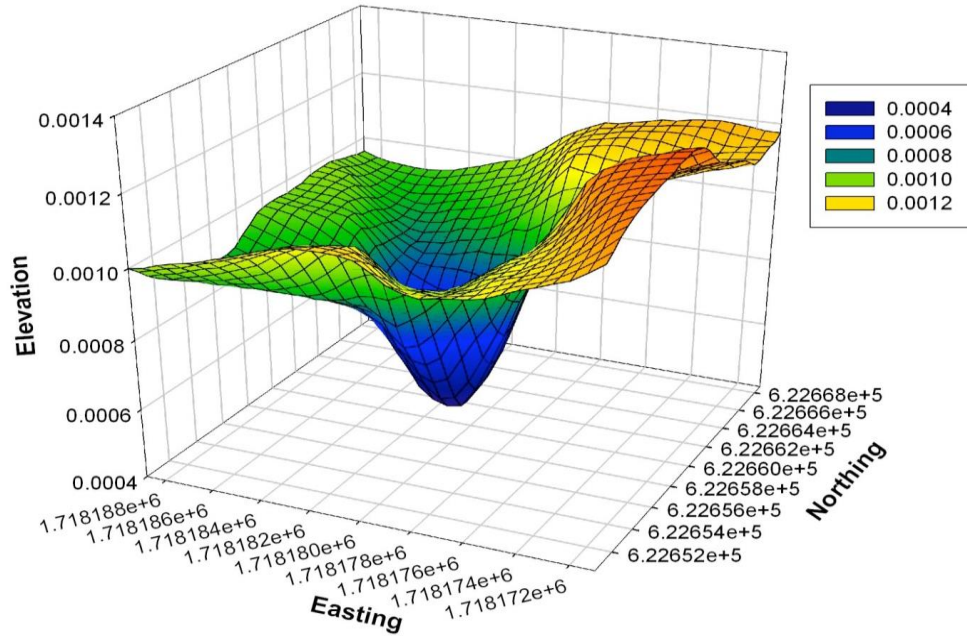
Although an MLS and a TLS can provide long scanning range—more than 1,000 m (even the range of some special TLSs is larger than 5,000 m)—their reliabilities, however, may not satisfy the basic requirements for pavement inspection because longer distance always results in lower point density, accuracy, and precision. As a result, only the original data output from the first several dozen or 100 m can be used for data post-processing, so its measuring speed is usually approximately 0.15 mph. Furthermore, the scan rate of LiDAR varies considerably depending on the working theory (e.g., time of flight, phase, or waveform processing), manufacturer, and models. Basic models have scan rates ranging from 25,000 pts to 120,000 pts, whereas upgraded models have scan rates up to 1,000,000 pts—of course at greater cost.

Table 3 summarizes recent research studies using LiDAR systems for pavement inspection, including the software used.

**Table 3. Research focusing on using LiDAR systems for pavement inspection**

<b>Researchers</b>	<b>LiDAR Device</b>	<b>Applications</b>	<b>Software</b>
Chang et al. 2006	Mensi GS100	IRI	PointScape, RealWork
Johnson et al. 2010	Lecia ScanStation II	Curling and warping, IRI	Lecia Cyclone
Amadori 2011	Riegl VMX-250	Pavement resurfacing	EarthView
Chin 2012	Riegl VZ-400 3D	Cross slopes, IRI	ProVAL
Tsai and Li 2012	HD 3D laser profiler	Crack detection	N/A

The original data output is quite similar for all LiDAR devices, and the final deliverable output depends primarily on the software used for post-point cloud processing, such as data filtering, noise removal, calibration, adding red-green-blue color, 3D visualization, and surface profile development. Figure 24 illustrates a final output from the research conducted by Johnson et al. (2010) that used a commercial TLS to monitor curling and warping for a newly constructed concrete pavement in South Carolina.



Johnson et al. 2010

**Figure 24. Curling and warping measurement by using TLS**

In that study, Leica Cyclone software was used to process the point cloud data and remove noise, with Microstation then used to create a triangulated irregular network for each point cloud to interpolate the coordinates at multiple points (Johnson et al. 2010). A 3D plot from the exported data was then generated using graphing software. As Figure 24 shows, the amount of curling and warping captured is approximately 0.0006 ft (0.2 mm). This value is so small as to be nearly impossible to detect using previously described conventional methods (Johnson et al. 2010).

### 2.3 Summary of Literature Review Results

Measurement of the actual degree of curling and warping taking place in concrete pavements is of paramount significance in developing performance measures and critical threshold magnitudes as well as gaining better understanding of their relationship to diurnal and seasonal temperature/moisture changes and long-term pavement performance. There is currently, however, no standardized method to measure curling and warping in practice. Table 4 summarizes existing devices that have been explored in experimental research studies for measuring curling and warping.

It can easily be seen that the majority of methods are quite expensive and involve complex procedures in performing calibration, operation, and data interpretation. Other less expensive methods are usually time consuming. There is, therefore, a critical need for development of a simple, portable, economic, reliable, accurate, and rapid curling and warping measurement device. To effectively develop such a portable curling and warping device capable of satisfying such needs, design criteria based on literature review results must first be developed.

**Table 4. Summary of currently available devices for measuring slab curling behaviors (prices available until July 2015)**

<b>Device</b>	<b>Speed (mph)</b>	<b>Resolution (in.)</b>	<b>Road Closure Required</b>	<b>Price</b>	<b>Min. Number of People</b>	<b>Difficulty of Operation</b>	<b>Portable</b>	<b>Limitations</b>
Rod and Level	0.006	0.005	Yes	\$240	2	Simple	No	• Intensively time and labor consuming
Straight Edge	0.05	0.0625	Yes	\$150	1	Simple	Yes	• Fixed beam length (5.7 to 16 in.) • Not correlated with other methods
Dipstick Profiler	2	0.005	Yes	\$4,500	1	Medium	Yes	• Results not reliable when sampling interval is short
Profilograph	3	0.01	Yes	\$8,000	2	Medium	No	• Limited wavelength • Does not measure true profile
LVDT System	N/A	infinite	No	\$4,500*	N/A	Medium	No	• Has to be installed in pavement • Sensor survivability issues in concrete • Fixed single point measurement • Installation and data-logger are costly
Digital Indicators System	N/A	0.0001	Yes	\$1,300*	N/A	Simple	Yes	• Usually used before traffic opening • Single point measurement • Time consuming installation
RTRRMs	50	0.125	No	\$8,000	1	Complex	No	• Frequent and complex calibration • Results not reproducible and not stable with time • Does not measure true profile
Walking Profilometer	2.5	0.0001	Yes	\$30,000	1	Medium	No	• Easily affected by external factors
Merlin	2.5	N/A	Yes	\$200	1	Medium	No	• Does not measure true profile • Results are IRI only
ALPS 2	13	0.0001	Yes	\$10,000	1	Complex	No	• Complex data processing
High-Speed Profiler	70	0.001	No	\$50,000	1	Very Complex	No	• Not accurate when speed < 10 mph • Difficult data processing
Lightweight Profiler	30	0.001	Yes	\$40,000	1	Complex	No	• Difficult data processing
TLS	0.15	0.001	No	\$60,000	1	Complex	No	• Difficult data processing
MLS	75	0.001	No	\$600,000	1	Very Complex	No	• Difficult data processing • Extremely high price

\* Assume three LVDTs or digital indicators to measure curling and warping at slab corners and mid-edge (price includes data-loggers)

### **3. DESIGN APPROACH OF THE ISU PORTABLE CURLING AND WARPING MEASUREMENT DEVICE**

#### **3.1 Design Criteria**

Curling and warping-induced slab curvature is primarily upward because of long-term dry shrinkage characteristics (Guo and Marsey 2001, Van Dam 2015). This upward curvature (most noticeable at PCC slab corners) can be up to 1 in. (2.5 cm). In addition, when curl is less than 0.25 inch, the cracking is usually not so excessive as to disqualify a PCC slab (Suprenant and Malisch 1999). As a result, the curling and warping measurement device developed should be able to measure the curvature in a range of at least 0.25 inch to 1 inch in the field. Although existing methodologies may satisfy the basic requirements for measurement of magnitude of curling and warping for in-service concrete pavements, they all exhibit certain limitations such as high initial or operational cost, inconvenience, low accuracy, or difficulty in field operation, all of which may inhibit their use in routine inspection for QC and QA of concrete pavements. Based on literature review results presented in the previous sections, the design criteria for a new portable device could be enumerated.

Because the device is intended to be portable, it should be easily carried by one adult, meaning that the weight of the device should not be more than 25 pounds and its size should be as small as possible. Measurement time should not be greater than 10 minutes for obtaining 5 points from one edge to the other of a concrete slab. Methodologies involving avoidance of road closure, however, seem to always involve expensive laser scanning or presensor instrumentation before concrete placement, so eliminating road closure is not a mandatory design requirement. The summary of design criteria is listed as follows:

- Provide true deflection profile measurement of pavement
- Size of device small enough that it can be transported easily to the field
- Weigh less than 25 pounds so an adult can easily carry and set it up
- Easy to operate without special training
- Quick setup and measurement (time  $\leq$  10 minutes)
- Resolution greater than 0.25 inch
- Available measuring range at least 0.25 inch to 1 inch
- Repeatable results
- No complex calibration and calculation requirements
- Economical

#### **3.2 Development of First-Generation Prototype**

The first-generation prototype of the newly designed curling and warping measurement was developed and fabricated based on the stated design criteria. This device is a static pavement deflection-profiling instrument that sets up a tightened string over a concrete slab surface and measures mid-chord deflection of the pavement. Readings can be taken easily at random intervals along the string so that an overall pavement deflection profile can be developed.

Figure 25 includes images from different views of the first generation of this device.



**Figure 25. First generation of ISU curling and warping device: front view (top left), back view (top right), and side view from head (bottom)**

The images show that the device consists of two main columns (the black pieces shown in Figure 25) and one steel measuring gauge (see Figure 26).

For convenience of description, the two columns are divided into “column A” and “column B”; column A is the lower black frame in Figure 25 (top left) and column B is the upper one. In Figure 25 (top right), the order of columns A and B is reversed. Figure 25 (bottom) shows a side view from the heads of the two columns.

Columns A and B of the device were made of 21-inch-long 2- by 2-inch square hollow-section steel tubes 0.1 inch in thickness. Two 30-inch-long steel legs were screwed to the head of each column to support the columns standing at the slab edge. Steel chains were used to connect the legs and columns together and to hold the legs when they were opened. Aluminum rollers were

pinned on the metal plates welded to the columns to enable adjustment of the string during measurement.

As seen in Figure 25, column A has two rollers; one is 3 inches in diameter and another is 4 inches in diameter. Column B has only one 3-inch-diameter roller. The 4-inch-diameter roller in column A is a U-groove solid wheel equipped with a 4-inch-long crank. The tread diameter is 3.5 inches and the width of the U groove is 1.6 inches. The string is a 0.06-inch-diameter stainless steel rope that can hold up to a 500-pound force. It is twined around the 4-inch-diameter roller and hooked up between the two rollers in column A by a spring hook. The string is about 30 feet long, enough to measure a concrete slab.

Three small holes 0.25 inch in diameter were drilled in both flanges of the 4-inch-diameter roller, and matching holes were drilled on each of the soldered metal plates at corresponding positions. When the holes are aligned by rotating the crank, a steel bar of the same diameter can be inserted to lock them together.

With respect to the 3-inch-diameter roller in column A, a small groove 0.06 inch in depth and width was cut to restrain the lateral motion of the string during measurement. For column B, the roller pinned is exactly the same as the one in column A. When the string is drawn toward the roller in column B, it can be hooked to the bottom of a bolt fastened by an 8-inch-long handle at the head. The bolt can be moved up by adjusting the handle so the string will be tightened after the larger roller in column A is pinned and locked. In addition to the columns, a right-angle triangular prism measuring gauge was made to measure the gap between the string and the pavement surface. This gauge has a step-shaped slope 10.25 inches in length and 1 inch in height. The step-shaped slope is evenly divided into 20 divisions, so the height difference of adjacent scales is 0.05 inch. The scales are marked from 1 to 20; 1 represents 0.05 inch and 20 represents 1 inch in height, as shown in Figure 26.



**Figure 26. Triangular measuring gauge**



### 3.3 Principle of Operation

This device has two columns standing on the opposite edges of a concrete slab where the level of curling and warping is to be measured. The distance between the two columns is the length of this slab. When the string is placed over the pavement surface and tightened by adjusting rollers and handle in columns A and B, the gap created between the string and the pavement surface corresponds to the upward pavement deflection. The instrument will measure mid-chord deflection by placing the lowest scale of the triangular measuring gauge on the pavement surface just under the string. The gauge is pushed to laterally pass through the string until it touches the string. The scale position at which the string is touched will be recorded as mid-chord deflection. This scale position can be easily converted to inches by multiplying the scale number by 0.05 inch, and the lateral location of the measured point can be recorded using a tape. Detailed operational steps are as follows:

1. Place column A in the middle of the slab edge and adjust its two legs to make it upright.
2. Place column B at the opposite side and stand it upright by adjusting its two legs.
3. Unhook the string from the 4-inch-diameter U-groove wheel of column A and drag it through the groove in the 3-inch-diameter roller.
4. Keep dragging until the string passes through the bottom of column A, then draw the string to pass through the roller of column B.
5. Hook the string to the bolt of column B.
6. Adjust the crank of the U-groove wheel of column A to store the extra string back on the wheel, and pin the steel bar into the holes to lock the wheel.
7. Adjust the handle on the head of column B to tighten the string.
8. Use the measuring gauge to measure the gap between the pavement surface and the string, and use a tape to record the lateral distance of the point measured.

## **4. DEVICE ENHANCEMENTS AND EVALUATIONS**

### **4.1 First-Generation Prototype**

The prototype of the first generation of the ISU curling and warping measurement device, shown in Figure 25, has a total weight of approximately 24 pounds. The height of the two main columns is 21 inches, and they can be placed into a small bucket to be transported in the field. Setup processes, including placing the tape to record locations of measured points, take approximately 3 minutes. Measurement of one point requires about 2 seconds. Since there is no need to measure the entire pavement deflection profile for curling and warping, 5 to 9 data points at critical locations should be sufficient, so it will take less than 1 minute to completely measure a concrete slab. After laboratory testing and assessing the prototype of this instrument, it was found that several improvements could be made to make it lighter, smaller, and easier to use. Detailed modifications are presented in the next sections.

### **4.2 Second-Generation Prototype**

#### *4.2.1 Device Enhancement*

After assessing the first-generation ISU curling and warping device in the laboratory, it was found that the legs for keeping the columns upright at slab edges were not necessary, so modifications were made to disassemble the 30-inch-long legs and reduce the total weight. Two much smaller feet 2 inches in length (see Figure 27 upper left) were added laterally at the bottom at a certain angle to maintain column balance at the edges if the pavement surface was uneven.





**Figure 27. Improvements made for second generation of ISU curling and warping measurement device: small feet (upper left), anchor (upper right), and additional holes on the flanges of U-groove wheel in column A (bottom)**

Additionally, to keep the instrument standing firmly at the slab edges, two small anchors (1.5 inches long) were soldered vertically underneath the bottom of each column, as shown in Figure 27 (upper right). These anchors were designed to be inserted into pavement joints so that the columns could be stuck into the joints to restrain their movement. Because a joint is usually cut to be 0.4 to 0.6 inch wide for cracking control and joint sealant, the anchor was 0.1 inch in thickness. Cuts were also made in the middle of the anchors to leave space for the string to pass straight through. The columns and the handle in column B were cut to be 16 inches and 6 inches long, respectively, reducing the total weight of the instrument by 5 pounds. At column A, the 4-inch-diameter U-groove wheel was moved down and the hook in the middle was moved up to create more spacing for cutting.

Additional holes were then drilled in the flanges of the U-groove wheel to make it more adjustable (see Figure 27 bottom). This will reduce the use of the iron handle of column B to adjust string tension. Figure 28 shows an overview of the second-generation device after these improvements.



**Figure 28. Overview of second generation of ISU curling and warping measurement device**

The heights of the columns were reduced to 15 inches and the total weight was reduced to 20 pounds.

#### *4.2.2 Field Test for Device Evaluation (October 24, 2014)*

A field test was conducted on October 24, 2014, to assess the performance of the second-generation device in situ and seek further improvements. A newly paved ISU campus PCC parking lot was selected as the test location. Figure 29 is a map view of the test site located on the east side of the ISU campus between 13th Street and University Blvd.

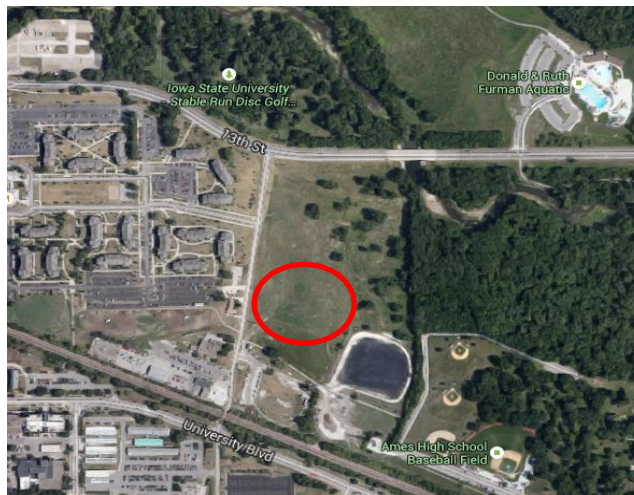


Image ©Google 2014

**Figure 29. Field test site on ISU campus**

Grass is shown at the test location on this map because the newly constructed parking lot had not yet been updated in the Google Map display.

Two field tests were conducted: (1) at 10:00 a.m. with 58°F ambient temperature and 93% ambient relative humidity (RH), and (2) at 5:30 p.m. with 74.4°F ambient temperature and 75% ambient RH. Because curling and warping is caused by different temperature and moisture gradients throughout the PCC slab depth, temperature and RH variation is needed for meaningful testing. The selected slab was located in a driveway at the back of the parking lot because pavement deflection there would be magnified under frequent vehicle loads. The tested PCC slab was 12.2 feet long and 10.5 feet wide with a diagonal length of approximately 15.5 feet.

Before the morning test, two small holes were made at the joint centers to insert the column anchors. The string was then unhooked from column A and pulled through the roller of column B. The string was hooked to the bottom of the bolt and the steel bar then inserted into the hole of the U-groove wheel to lock column A. The handle of column B was then adjusted to firmly tighten the string. Figure 300 illustrates the finalized set-up of the second-generation ISU curling and warping measurement device in the field.



**Figure 30. Field test on October 24, 2014: vertical view (left) and horizontal view (right)**

A measuring tape can be seen spread out along the string to record locations of measured points. Because of heavy wind on that day, a wooden box was placed on the tape to restrain its movement. A portable temperature sensor was also provided to record the pavement-surface temperature, 61.7°F at that time. The whole setup process took approximately 4 minutes.

ASTM E1364-95 (ASTM 2012a) recommends a maximum measuring interval between two data points of 1 foot for Class 1 resolution (0.005 inch) and 2 feet for Class 2 resolution (0.01 inch) when performing roughness assessment. For curling and warping, Class 2 resolution already satisfies the basic measuring requirement, so a 2-foot interval is sufficient. In most cases, however, there are critical curling and warping locations, so five measurements at even intervals along the profile are recommended in the field.

In this test, measurements were taken every 1 inch for device assessment purposes only; five measurements near the two ends (10 feet and 11.9 feet), at the center (6.1 feet), and at middle points between the ends and center (3 feet and 8 feet) were taken first to obtain a raw pavement

deflection profile. Figure 31 shows the measurements taken at these positions; it took less than 0.5 minute to obtain this data.



**Figure 31. Profile measurements: at the joint (left) and at the center (right)**

Other measurements were taken at one-inch intervals, the whole process taking approximately 10 minutes.

The afternoon test followed the same procedures at the same positions. The pavement deflection profiles captured both in the morning and in the afternoon are shown in Figure 32.

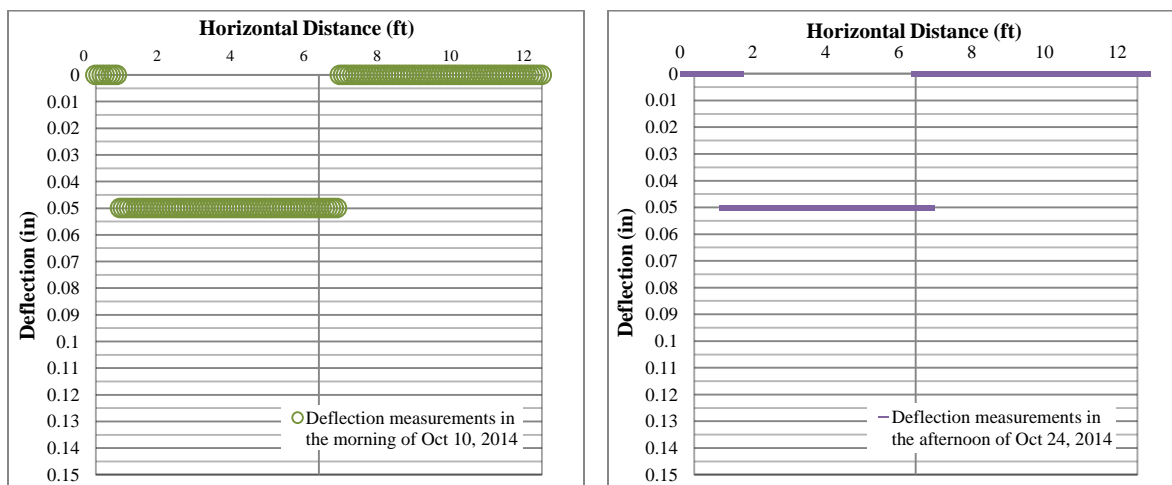


**Figure 32. Pavement deflection profiles measured on October 24, 2014: profile measured in the morning (left) and profile measured in the afternoon (right)**

A comparison between the two profiles is also shown in Figure 33.



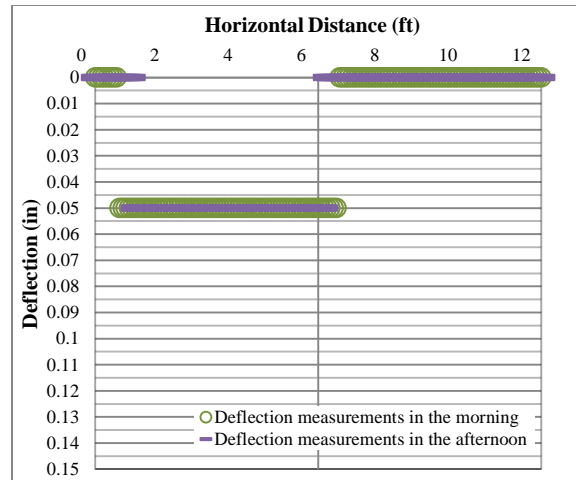


**Figure 33. Comparison between morning and afternoon measurements on October 24, 2014**

In Figure 32 and Figure 33, the string was used as a datum line for mid-chord deflection measurement. The deflection can be used to represent how much the slab curled/warped at this point with respect to the lowest point, usually at about the slab center. According to Figure 32, the slab indicated a left-skewed upward curvature, and maximum deflection was found at joints (0 foot and 12.2 feet) on the horizontal axis, fully consistent with the general phenomenon of curling and warping behavior of concrete slabs in the field.

The maximum upward curling and warping captured in the morning by the triangular measuring gauge was 0.05 inch along the pavement longitudinal profile from 0 to 7 inches and 6.7 to 12.2 feet. In the afternoon, maximum upward curling and warping was also 0.05 inch but along the 0–1-inch and 6.3–12.2 -foot profile sections.

A comparison of the profiles measured in the morning and in the afternoon is shown in Figure 33; it reveals no significant observed difference between morning and afternoon measurements. Most regions of the two profiles looked identical and were overlapped with each other. It still can be seen, however, that the slab had more parts curled/warped to 0.05 inch in the afternoon because 83 of 146 measurements were on the x-axis in the afternoon compared with 75 of 146 measurements on the x-axis in the morning. This phenomenon is fully in agreement with the generally expected situation in the field where more warping is expected in the afternoon due to dry shrinkage.

This test validated the feasibility of using this instrument to capture curling and warping behaviors of concrete pavement in the field. The instrument provided easy and relatively fast operation and reliable results. It was realized, however, that the string was not fully pushed to the pavement surface underneath the columns because of spaces between the feet and the column. The bottoms of the feet were intentionally soldered 0.06 inch deeper than the bottom of the column to avoid severe string abrasion from unevenness caused by the string diameter. In this way, some space was created when the columns were inserted into the joints, possibly inducing bias if the string was not held down to the pavement surface very firmly. Moreover, the degree of

curling and warping was very small, so it was difficult for the triangular measuring gauge to capture continuous small changes along the pavement longitudinal profile.

### **4.3 Third-Generation Prototype**

#### *4.3.1 Device Enhancement*

Previous field tests indicated that the string was not firmly pushed to the pavement surface and continuous curling and warping changes were too small to be adequately captured by the measuring gauge, so accessories were used to assist in the measurement (see Figure 34).



**Figure 34. Accessories (clips and pins)**

These accessories included two clips and two small pins. The clips were placed under the bottom of the columns so that the string would be held down to the pavement surface more firmly. The small pins were placed under the string near the two columns to create distance between the string and the pavement surface. In this way, the results measured both with and without the pins could be compared to validate the repeatability of this instrument, and errors due to bumps or downward curvature in some parts of the slab with elevations higher than the elevations of two ends (columns A and B) could be eliminated.

A laboratory demonstration using the clips and pins is shown in Figure 35.



**Figure 35. Demonstration of using accessories in the laboratory**

A field test was conducted on November 10, 2014, to evaluate effectiveness of these accessories. A measuring gauge with higher resolution was also substituted and another field test conducted on April 10, 2015, to evaluate the effectiveness of the measurement device.

#### *4.3.2 Field Test for Device Evaluation (November 10, 2014)*

Two sets of field tests were conducted in the morning and afternoon of November 10, 2014, to test the repeatability of the instrument and try the new accessories shown in Figure 34. The morning test was conducted at 9:00 a.m. at 46°F ambient temperature and 80% ambient RH. The pavement surface temperature measured by an infrared temperature gun was 41°F. In the afternoon, ambient temperature and pavement surface temperature were 58°F and 54.6°F, respectively, and the RH had decreased to 60%. The slab tested was the same one tested on October 24, 2014.

Curling and warping along diagonal lines of the slab were also measured in the morning test. Figure 36 and Figure 37 illustrate the test in the field using the added accessories for longitudinal and diagonal profile measurement, respectively.



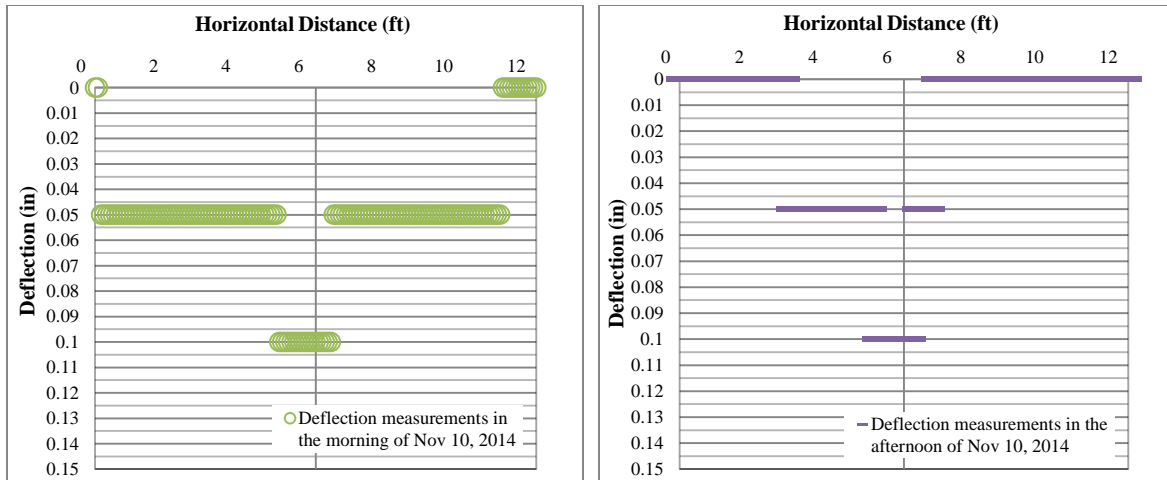
**Figure 36. Field test on November 10, 2014: setup overview (left) and clips used in the ends (right)**



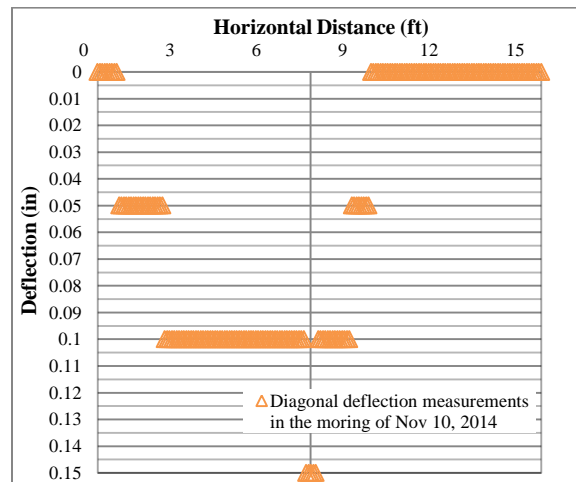
**Figure 37. Diagonal profile measuring on November 10, 2014**

Figure 38 and Figure 39 also illustrate the captured pavement longitudinal and diagonal profiles, respectively.





**Figure 38. Pavement deflection profiles measured on November 10, 2014: profile measured in the morning (left) and profile measured in the afternoon (right)**



**Figure 39. Diagonal profile measured in the morning of November 10, 2014**

A comparison of longitudinal profiles developed from the morning and afternoon tests is shown in Figure 40.

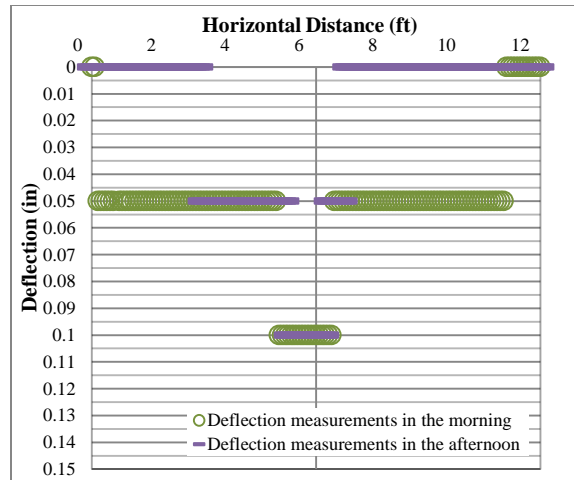


**Figure 40. Comparison between morning and afternoon measurements on November 10, 2014**

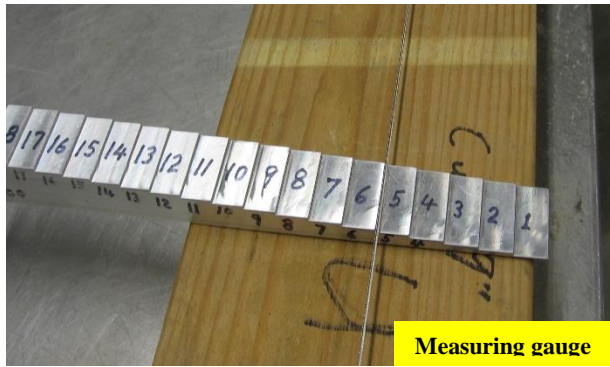
As shown in Figure 38 and Figure 39, the maximum curling and warping was 0.1 inch in the middle of the joints for the longitudinal profile and 0.15 inch for the diagonal pavement deflection profile at the slab corners. These results show reasonable agreement with common sense indicating that slab corners should experience the highest deflection. Additionally, all measurements taken with and without the pins under the string were the same after calibrating the displacement to account for the pins.

Figure 40 provides a comparison of the morning and afternoon test results. It indicates that diurnal changes of curling and warping are very small. Nevertheless, there was still more curling and warping observed when compared to the results observed on October 24, 2014. It was also found that the slab had more parts curled and warped in the afternoon; this closely matched the observations on October 24, 2014. After this test, however, it was noticed that the triangular measuring gauge used made it difficult to capture small deflection changes between closely adjacent measured points in newly constructed pavement. As a consequence, the use of alternative higher-resolution rulers was recommended.

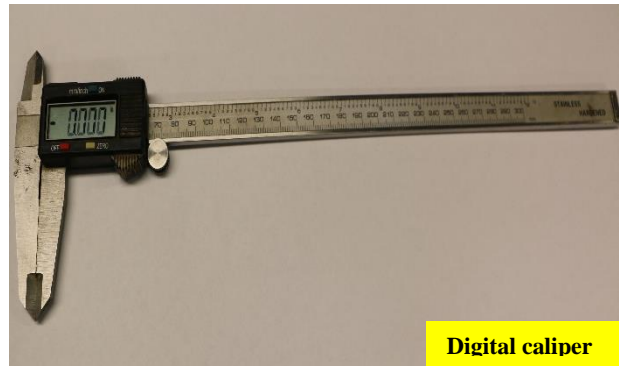
#### *4.3.3 Comparisons of Alternative Rulers*

As mentioned earlier, there is a concern about resolution obtained using the triangular measuring gauge developed when the magnitude of curling and warping is very small, particularly in newly constructed concrete pavement. Furthermore, the results measured by the triangular measuring gauge may be affected by pavement surface irregularities.

As a result, several alternative rulers (see Figure 41) were compared with respect to measuring range, price, resolution, ease of use, and total time needed to take five basic point measurements.



Measuring gauge



Digital caliper



Depth micrometer



Image: © Amazon

Digital indicator



Image: © Amazon

Digital dial gage



Image: © Amazon

Digital Z-height gauge



Digital tread depth gauge



Digital height gauge

Figure 41. Rulers evaluated in this study

Table 5 summarizes results for rulers available in the market and the ISU laboratory.

**Table 5. Comparison of rulers for measuring curling and warping**

<b>Name</b>	<b>Max. Range</b>	<b>Resolution</b>	<b>Time*</b>	<b>Cost</b>	<b>Limitations</b>
Triangular measuring gauge	1 in.	0.05 in.	10 s	N/A	<ul style="list-style-type: none"> <li>• Does not have enough resolution to capture small deflection change</li> </ul>
Digital caliper	6 in.	0.005 in.	30 s	\$10	<ul style="list-style-type: none"> <li>• Hard to operate in the field due to “large head” of the ruler</li> </ul>
Depth micrometer	75 mm	0.005 mm	1 min	\$247	<ul style="list-style-type: none"> <li>• No digital readings</li> <li>• Time consuming</li> <li>• Expensive</li> </ul>
Digital indicator	1–16 in.	0.0005 in.	30	\$24	<ul style="list-style-type: none"> <li>• Small basic range (1 in.)</li> <li>• Range depends on rods; extra cost to obtain a longer one</li> </ul>
Digital dial gauge	0.5 in.	0.00005 in.	1 min	\$72	<ul style="list-style-type: none"> <li>• Small range</li> <li>• Time consuming</li> <li>• Relatively high price</li> </ul>
Digital Z-height gauge	6 in.	0.0005 in.	40 s	\$42	<ul style="list-style-type: none"> <li>• Relatively high price</li> <li>• Not portable</li> </ul>
Digital tread depth gauge	1 in.	0.001 in.	10 s	\$8	<ul style="list-style-type: none"> <li>• Small range</li> </ul>
Digital height gauge	3 in.	0.001 in.	10 s	\$20	N/A

\* Time is estimated or measured by taking five measurements along the string of this instrument.

Based on the comparisons, the rulers’ “digital tread depth gauge” and “digital height gauge” were selected due to their small size, high resolution, electronic reading, fast operation in the field, and competitive prices.

Figure 42 compares and demonstrates the use of two alternative rulers and triangular measuring gauge at the same position.



**Figure 42. Comparison of the alternative rulers in the laboratory**

Note that the results from the digital tread depth gauge and digital height gauge required subtracting the diameter of the string, 0.06 inch as mentioned earlier. Figure 43 shows that the true displacements with pins between the string and the surface of the wood box—measured by the measuring gauge, the digital tread depth gauge, and the digital height gauge—were 0.5 inch, 0.538 inch, and 0.538 inch, respectively.

#### *4.3.4 Field Test for Device Evaluation (April 10, 2015)*

Figure 43 shows results from a field test conducted on April 10, 2015, on the same concrete slab along the mid-edge longitudinal profile.

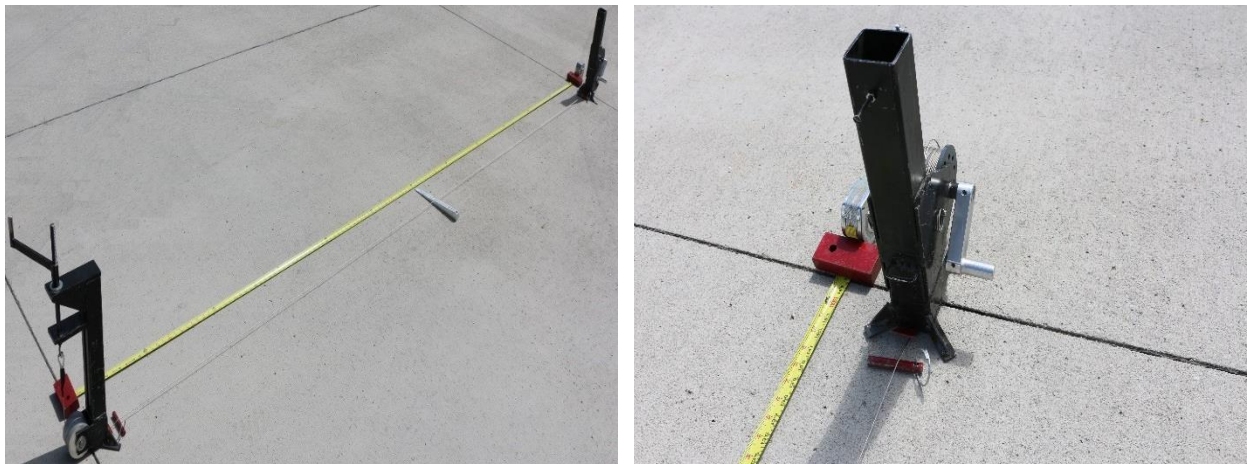


**Figure 43. Field test on April 10, 2014: setup overview (left) and pins used underneath the string in the ends (right)**

This test was conducted at 9:30 a.m. at ambient conditions of 47°F and 61% RH and again at 4:00 p.m. at ambient conditions of 56°F and 37% RH, respectively. The pavement surface temperatures measured with an infrared temperature gun were 45.3°F in the morning and 69.6°F



in the afternoon. Two small iron bricks were used to restrain tape movement due to heavy wind; pins were placed under the string near its ends. A comparison using the alternative rulers in situ is given in Figure 44.



**Figure 44. Comparison of the three rulers in the field**

Figure 45 compares test results from the three rulers taken in the morning and the afternoon.

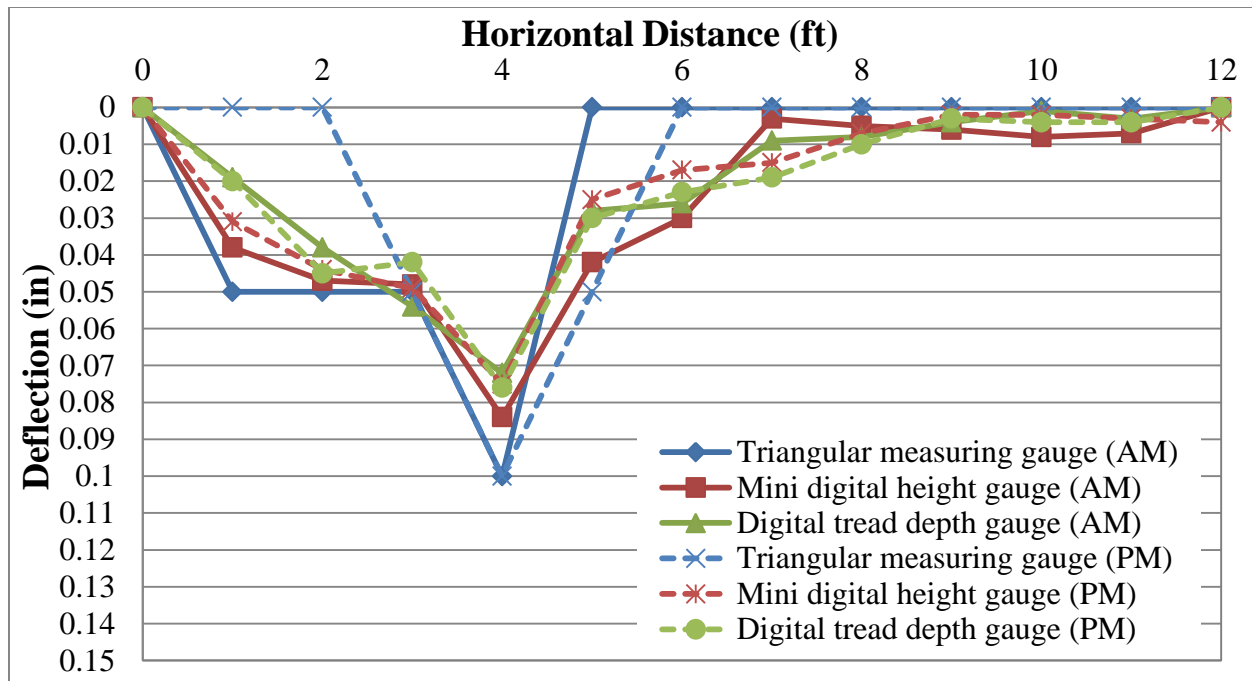


**Figure 45. Comparison between morning and afternoon measurements on April 10, 2015**

The measuring interval is 1 foot at this time rather than the 1 inch used in previous tests. This figure shows that the profiles captured by the electronic rulers have more curved and reasonable shapes due to their higher resolution compared to the profiles measured by the triangular measuring gauge. Furthermore, this figure still indicates a left-skewed pavement curvature consistent with previous results, and all measurements taken by the three rulers look similar. The deflection measured using the digital height gauge and digital tread depth gauge indicate a slightly smaller deflection than that from the triangular measuring gauge, probably because the two rulers slightly pushed the string down during measurement (see Figure 44).

It is therefore recommended that measurements be taken gently when using the two electronic rulers. The maximum upward curling and warping observed were 0.1 inch, 0.84 inch, and 0.072 inch in the morning and 0.1 inch, 0.075 inch, and 0.076 inch in the afternoon from triangular measuring gauge, digital height gauge, and digital tread depth gauge measurements, respectively. It should also be noticed that displacements measured by the two electronic gauges included subtraction of the string diameter from displacements induced by the pins, as previously mentioned. They also must be zeroed each time before measuring.

These results indicate that the digital tread depth gauge and digital height gauge can provide fast and reliable curling and warping measurements. The time required for taking five measurements is less than 1 minute in the field. Field experience, however, recommends use of the digital height gauge because it's faster and easier to operate. Digital tread depth is susceptible to pavement surface irregularity such as small sunk potholes or bulged aggregates because of its tiny contact point at the end of the ruler.

## **4.4 Fourth-Generation Prototype**

### *4.4.1 Device Enhancement*

It was realized that some improvements to reduce the size and weight of the instrument were still possible, so final modifications to make this instrument smaller and lighter were accomplished. The height of column A was reduced to 12 inches by cutting the part above the flexible spring. Column B length was reduced to 12 inches by removing some pieces in the middle. The handle length at the head of column B was reduced to 3 inches long. As a result, the total weight was reduced to 18 pounds. The anchors were also cut at a certain angle to make them sharp and abraded as well as thinner so they could be inserted into joints easily.

The steel string was also replaced by a 30-foot-long cord 0.008 inch in diameter made from woven Technora, a very high-strength, low-stretch, and abrasion-resistant material. The new string had a breaking strength of 450 pounds, similar to that of the steel string previously used but with a lower weight and price. Figure 46 illustrates the improvements of the fourth-generation instrument after modifications, and Figure 47 shows finalized columns A and B.



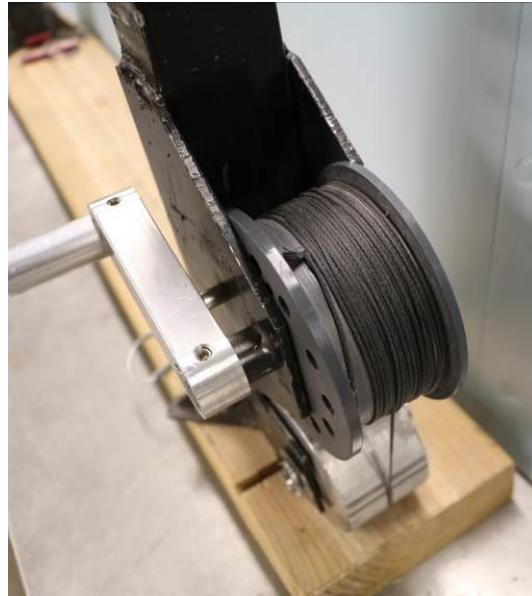


**Figure 46. Improvements made for fourth generation of ISU curling and warping measurement device: shorter head of column A (top left), shorter handle of column B (top right), sharp anchor (bottom left), and replaced cord (bottom right)**

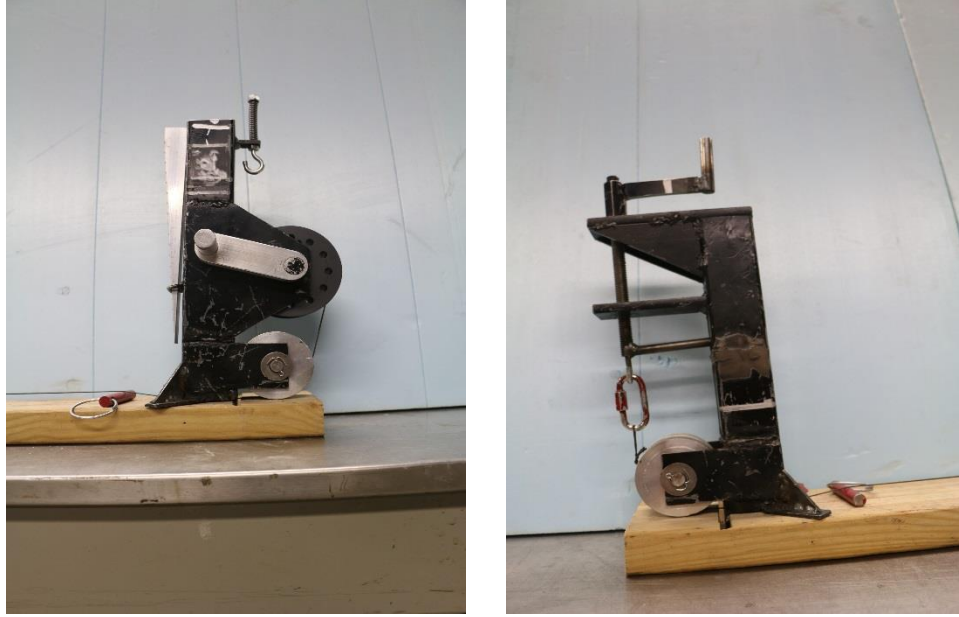


**Figure 47. Fourth generation of ISU curling and warping measurement device: column A (left) and column B (right)**

#### *4.4.2 Field Test for Device Evaluation (June 20, 2015)*

This test was conducted on June 20, 2015, to assess the latest version of the ISU curling and warping device on the same concrete slab previously used. As in the case of previous tests, both morning and afternoon measurements were taken. The first test was performed at 10:00 a.m. with 72°F ambient temperature, 71°F surface temperature, and 78% RH. The second test was performed at 4:30 p.m. with 83°F ambient temperature, 85°F surface temperature, and 68% RH. Both the triangular measuring gauge and the digital height gauge were used, as shown in Figure 48.



**Figure 48. Field test on June 20, 2015: setup overview (left) and measuring using rulers (right)**

Figure 49 shows the calibrated results with pins from these tests.

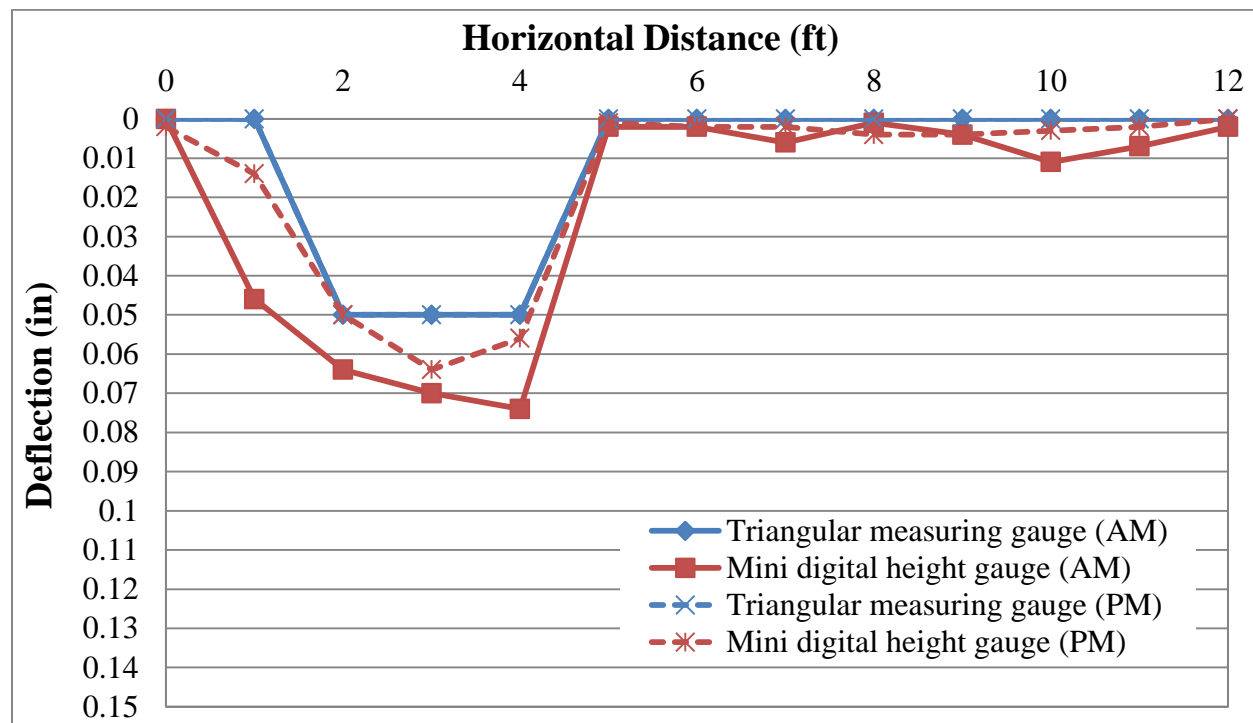


**Figure 49. Comparison between morning and afternoon measurements on June 20, 2015**

Figure 49 shows that the data measured from the morning and afternoon tests on June 20, 2015, exhibited similar trends to those previously observed. In the morning test, however, the maximum upward deflection became 0.074 inch, smaller than the 0.084 inch observed on the morning of April 10, 2015. This difference was because a heavy rain had occurred in the early morning of June 20, 2015, so the pavement surface was wetter than its bottom, reducing the magnitude of upward deflection due to induced downward curling and warping. From field observation, however, it was found that the woven Technora cord was occasionally slightly pushed down in the middle of the slab due to the force exerted by the digital height gauge. To reduce this bias, the triangular measuring gauge can be placed under the string and the measuring bar of the digital height gauge slightly adjusted (see Figure 48 right).

Another way for resolving this issue would be to continue using the steel string because it's much firmer and will not bend under the force of the digital height gauge. It is also recommended to always use the pins under the string during measurements just in case there is downward curvature at some parts of the concrete slab that has relatively higher elevation than the ends (e.g., column A and B).

#### 4.5 Summary of the Developed Prototype of Device

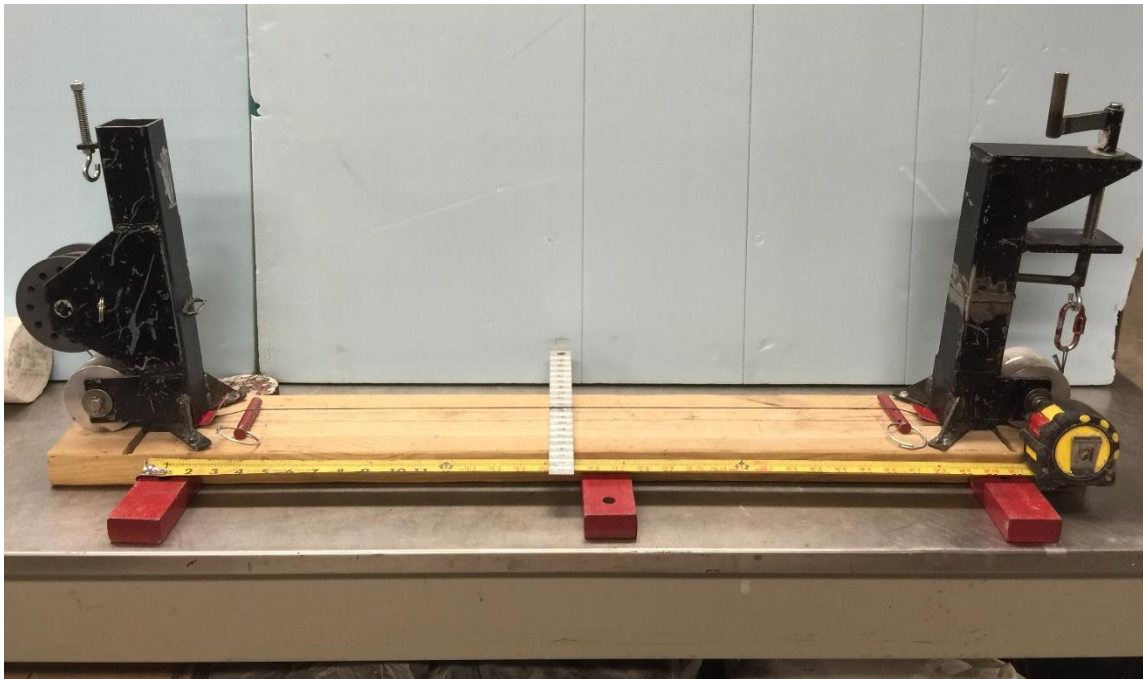
Based on a series of field tests, the accuracy and repeatability of the implementation of the finalized ISU curling and warping device satisfy the requirements of curling and warping

measurements in the field. The final version (fourth generation) of this instrument has two main columns 12 inches in height and weighs 18 pounds. The unit can be easily carried and used in the field by just one adult. Two levels of resolution (0.05 inch and 0.001 inch) can be achieved using a measuring gauge and/or digital height gauge, depending on project requirements and total degree of curling and warping. If the degree of curling and warping is small, the higher-resolution ruler should be used. The horizontal measuring range is 30 feet, depending on the length of string used; longer strings can be used if the slab is longer than 30 feet. The total cost of this instrument is approximately \$320, as shown in Table 6.

**Table 6. Cost of ISU curling and warping measurement device**

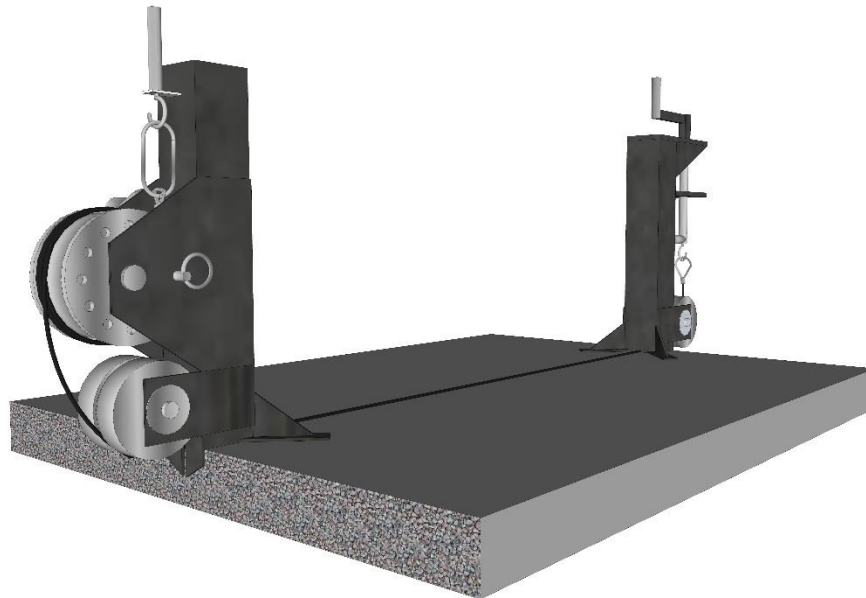
<b>Components</b>	<b>Cost (\$)</b>
String	10
Main columns	50
Accessories	20
Measuring gauge	20
Digital height gauge	20
Labor	200
<b>Total</b>	<b>320</b>

Figure 50 shows the final version of the instrument including all accessories.



**Figure 50. Final version (fourth generation) of ISU curling and warping device with all accessories**

Figure 51 is a 3D illustration of the instrument.



**Figure 51. Three-dimensional illustration of ISU curling and warping device**

Additional illustrations are included in Appendix A, Appendix B contains a schematic diagram of the device, and Appendix C contains an operation manual.

## 5. SUMMARY

The primary objective of this research was to develop an economic, portable, easy-to-use, and reasonably accurate curling and warping measurement device to be used for routine for QC and QA inspection of concrete pavements. The advantages of this device compared to other methods are as follows:

- This device has small size and relatively light weight for convenient transportation to the field.
- This device has comparable and flexible resolution (can be 0.001 inch or higher), depending on the rulers used.
- Compared to other available devices such as rod and level and straight edge, the ISU portable curling and warping measurement device has faster operational speed without intensive labor requirements (only one adult required). The device is much cheaper as well.
- Compared to profilers (both low-speed and high-speed profilers) and LiDAR systems, the ISU curling and warping device is much more portable and easier to operate. No special or complex training and software are required for device operation, data processing, and calibration.
- Compared to LVDTs and digital indicator-based curling and warping measuring systems, the ISU portable curling and warping measurement device can be used without preinstalled time-consuming and labor-intensive sensing systems. Many LVDTs and digital indicators have been limited in obtaining a comprehensive pavement deflection profile because of their single and fixed point measurement, whereas the ISU portable curling and warping measurement device can provide flexible measurement across the entire pavement.
- The device has a much lower cost, approximately \$320, compared to LVDT systems (at least \$3,000 for a single PCC slab, including installation cost and data-logger), digital indicator systems (\$2,000, including data-logger cost), profilers (at least \$5,000), and LiDAR systems (\$100,000, including software and data-processing cost). The price of this device could be further reduced to just \$100 if produced on an industrial scale.

In recent years there has been an increasing need for a standard device that is not only portable and economic but also simple and accurate for curling and warping measurement. The newly developed ISU curling and warping device can meet these demands; a series of field evaluation tests have demonstrated such feasibility.





## REFERENCES

- AASHTO. 2008. *Mechanistic-Empirical Pavement Design Guide: A Manual of Practice*. American Association of State Highway and Transportation Officials, Washington, DC.
- . 2013. *AASHTOWare Pavement ME Design*. American Association of State Highway and Transportation Officials, Washington, DC. [www.me-design.com/MEDesign/Index.html](http://www.me-design.com/MEDesign/Index.html). Last accessed December 30, 2015.
- AGL Laser. 2010. *Smart Rod*. [www.agl-lasers.com/](http://www.agl-lasers.com/). Last accessed December 30, 2015.
- Akkari, A. and B. Izevbekhai. 2012. *Composite Pavements and Exposed Aggregate Texturing at MnROAD: Cells 70, 71 and 72 Construction Report and Early Performance Evaluation*. Report MN/RC 2012-29. Minnesota Department of Transportation, St. Paul, MN.
- Amadori, J. 2011. *Mobile LiDAR and Cross-Slope Analysis*. Jason Amadori's LIDAR GIS blog, September 14, 2011, [jasonamadori.com/2011/04/27/mobile-lidar-and-cross-slope-analysis/](http://jasonamadori.com/2011/04/27/mobile-lidar-and-cross-slope-analysis/). Last accessed December 30, 2015.
- Ames Engineering. 2015. 8300 Portable High Speed Profiler, [amesengineering.com/products/8300-portable-high-speed-profiler/](http://amesengineering.com/products/8300-portable-high-speed-profiler/). Last accessed December 30, 2015.
- ARA, Inc., ERES Consultants. 2004. *Guide for Mechanistic-Empirical Design of New and Rehabilitated Pavement Structures*. Draft Final Report, NCHRP Project 1-37A. Transportation Research Board, National Research Council, Washington, DC.
- Armaghani, J. M., J. M. Lybas, M. Tia, and B. E. Ruth. 1986. Concrete pavement joint stiffness evaluation. *Transportation Research Record: Journal of the Transportation Research Board*. No. 1099:22–36.
- Armaghani, J. M., T. J. Larsen, and L. L. Smith. 1987. Temperature response of concrete pavements. *Transportation Research Record: Journal of the Transportation Research Board*. No. 1121:23–33.
- Asbahan, R. E. 2009. Effects of the built-in construction gradient and environmental conditions on jointed plain concrete pavements. PhD dissertation, University of Pittsburgh.
- ASTM. 2009. ASTM Standard E950-09. Standard test method for measuring the longitudinal profile of traveled surfaces with an accelerometer established inertial profiling reference. ASTM International, West Conshohocken, Pennsylvania. DOI: 10.1520/E0950\_E0950M-09, [www.astm.org/Standards/E950.htm](http://www.astm.org/Standards/E950.htm). Last accessed December 30, 2015.
- . 2010. ASTM Standard E1703-10. Standard test method for measuring rut-depth of pavement surfaces using a straightedge. ASTM International, West Conshohocken, Pennsylvania. DOI: 10.1520/E1703\_E1703M-10, [www.astm.org/Standards/E1703.htm](http://www.astm.org/Standards/E1703.htm). Last accessed December 30, 2015.
- . 2012a. ASTM Standard E1364-95. Standard test method for measuring road roughness by static level method. ASTM International, West Conshohocken, Pennsylvania. DOI: 10.1520/E1364-95R12, [www.astm.org/Standards/E1364.htm](http://www.astm.org/Standards/E1364.htm). Last accessed December 30, 2015.
- . 2012b. ASTM Standard E1082-90. Standard test method for measurement of vehicular response to traveled surface roughness. ASTM International, West Conshohocken, Pennsylvania. DOI: 10.1520/E1082-90R12, [www.astm.org/Standards/E1082.htm](http://www.astm.org/Standards/E1082.htm). Last accessed December 30, 2015.



- . 2012c. ASTM Standard E1215-93. Standard specification for trailers used for measuring vehicular response to road roughness. ASTM International, West Conshohocken, Pennsylvania, [www.astm.org/Standards/E1215.htm](http://www.astm.org/Standards/E1215.htm). Last accessed December 30, 2015.
- . 2012d. ASTM Standard E867-06. Standard terminology relating to vehicle-pavement systems. ASTM International, West Conshohocken, Pennsylvania. DOI: 10.1520/E0867-06R12, [www.astm.org/Standards/E867.htm](http://www.astm.org/Standards/E867.htm). Last accessed December 30, 2015.
- . 2012e. ASTM Standard E1170-97. Standard practices for simulating vehicular response to longitudinal profiles of traveled surfaces. ASTM International, West Conshohocken, Pennsylvania. DOI: 10.1520/E1170-97R12, [www.astm.org/Standards/E1170.htm](http://www.astm.org/Standards/E1170.htm). Last accessed December 30, 2015.
- Byrum, C. R. 2001. A high speed profiler based slab curvature index for jointed concrete pavement curling and warping analysis. PhD dissertation, University of Michigan.
- Caltrans. 2011. Chapter 15: Terrestrial laser scanning specification. *Caltrans Surveys Manual*. California Department of Transportation, Sacramento, California, [www.dot.ca.gov/hq/row/landsurveys/SurveysManual/15\\_Surveys.pdf](http://www.dot.ca.gov/hq/row/landsurveys/SurveysManual/15_Surveys.pdf). Last accessed January 2, 2016.
- Carter, J., K. Schmid, K. Waters, L. Betzhold, B. Hadley, R. Mataosky, and J. Halleran. 2012. *LiDAR 101: An Introduction to LiDAR Technology, Data, and Applications*. National Oceanic and Atmospheric Administration (NOAA) Coastal Services Center, Charleston, South Carolina, [coast.noaa.gov/digitalcoast/\\_/pdf/lidar101.pdf](http://coast.noaa.gov/digitalcoast/_/pdf/lidar101.pdf). Last accessed December 30, 2015.
- Cement Concrete & Aggregates Australia. 2006. *Curling of Concrete Slabs*, 59.167.233.142/publications/pdf/Curling.pdf. Last accessed December 30, 2015.
- Ceylan, H., D. Turner, R. O. Rasmussen, G. K. Chang, J. Grove, S. Kim, and C. S. Reddy. 2005. *Impact of Curling, Warping, and Other Early-Age Behavior on Concrete Pavement Smoothness: Early, Frequent, and Detailed (EFD) Study*. National Concrete Pavement Technology Center, Iowa State University, Ames, IA.
- Ceylan, H., S. Kim, K. Gopalakrishnan, and K. Wang. 2007. Environmental effects on deformation and smoothness behavior of early age jointed plain concrete pavements. *Transportation Research Record: Journal of the Transportation Research Board*. No. 2037:30–39.
- Ceylan, H., K. Gopalakrishnan, S. Kim, C. W. Schwartz, and R. Li. 2013. Global Sensitivity Analysis of Jointed Plain Concrete Pavement Mechanistic–Empirical Performance Predictions. *Transportation Research Record: Journal of the Transportation Research Board* No. 2367:113–122.
- Chang, G., R. Rasmussen, D. Merritt, S. Garber, and S. Karamihas. 2010. TechBrief: Impact of Temperature Curling and Moisture Warping on Jointed Concrete Pavement Performance. *Pavements*. Federal Highway Administration, Washington, DC. [www.fhwa.dot.gov/pavement/concrete/pubs/hif10010/index.cfm](http://www.fhwa.dot.gov/pavement/concrete/pubs/hif10010/index.cfm).
- Chang, J., K. Chang, and D. Chen. 2006. Application of 3D laser scanning on measuring pavement roughness. *Journal of Testing and Evaluation* 34 (2): 83–91.
- Chin, A. 2012. Paving the way for terrestrial laser scanning assessment of road quality. Thesis, Oregon State University.
- CST/berger. No date. *Rotation Lasers*. [www.cstberger.us/us/en/index.htm](http://www.cstberger.us/us/en/index.htm). Last accessed January 4, 2016.

- Cundill, M. A. 1991. *The MERLIN Low-Cost Road Roughness Measuring Machine*. TRRL Research Report 301. Department of Transportation, Crowthorne, Berkshire.
- Elkins, G. E., P. Schmalzer, T. Thompson, and A. Simpson. 2003. *Long-Term Pavement Performance Information Management System Pavement Performance Database User Reference Guide*. Report FHWA-RD-03-088. Federal Highway Administration, McLean, VA.
- FAA. 2009. *Advisory Circular—Standards for Specifying Construction of Airports*. AC No: 150/5370-10E. U. S. Department of Transportation Federal Aviation Administration. Washington, DC. [www.faa.gov/documentlibrary/media/advisory\\_circular/150-5370-10e/150\\_5370\\_10e.pdf](http://www.faa.gov/documentlibrary/media/advisory_circular/150-5370-10e/150_5370_10e.pdf). Last accessed December 30, 2015.
- FDOT. 2012. *Terrestrial Mobile LiDAR Surveying & Mapping Guidelines*. Florida Department of Transportation, Tallahassee, FL, [www.dot.state.fl.us/surveyingandmapping/documentsandpubs/20120823\\_TML\\_Guidelines.pdf](http://www.dot.state.fl.us/surveyingandmapping/documentsandpubs/20120823_TML_Guidelines.pdf). Last accessed December 30, 2015.
- FHWA. 2002. *A Synopsis on the Current Equipment Used for Measuring Pavement Smoothness*. [www.lpcb.org/index.php/documents/data-collection/roughness/11211-2002-usa-a-synopsis-on-the-current-equipment-used-for-measuring-pavement-smoothness/file](http://www.lpcb.org/index.php/documents/data-collection/roughness/11211-2002-usa-a-synopsis-on-the-current-equipment-used-for-measuring-pavement-smoothness/file). Last accessed January 4, 2016.
- FHWA. 2005. Appendix E: Measuring Pavement Roughness. In *Highway Performance Monitoring System Field Manual for the Continuing Analytical and Statistical Database*. Federal Highway Administration Office of Policy Information.
- Gerardi, T., D. Freeman, M. Freeman, R. O. Rasmussen, and G. Chang. 2007. *Airfield Concrete Pavement Smoothness—A Handbook*. Report IPRF-01-G-002-02-4. Programs Management Office, Skokie, IL.
- Guo, E. H. and W. Marsey. 2001. Verification of curling in PCC slabs at National Airport Pavement Test Facility. Pp. 15–29. In *Advancing Airfield Pavements, 27th International Air Transportation Conference, ASCE*. Chicago, IL.
- Harik, I. E., P. Jianping, H. Southgate, and D. Allen. 1994. Temperature effects on rigid pavements. *Journal of Transportation Engineering, ASCE* 120 (1): 127–143.
- Hiller, J. E. and J. R. Roesler. 2005. Determination of critical concrete pavement fatigue damage locations using influence lines. *Journal of Transportation Engineering, ASCE* 131 (8): 599–607.
- Huang, Y. H. 2004. *Pavement Analysis and Design*. 2d ed. Pearson Education, Inc., New Jersey.
- Janoff, M. S. and G. F. Hayhoe. 1990. The development of a simple instrument for measuring pavement roughness and predicting pavement rideability. pp. 171–183. In *Surface Characteristics of Roadways: International Research and Technologies*. Philadelphia, PA.
- Johnson, A. M., B. C. Smith, W. H. Johnson, and L. W. Gibson. 2010. *Evaluating the Effect of Slab Curling on IRI for South Carolina Concrete Pavements*. South Carolina Department of Transportation, Columbia, SC, and Federal Highway Administration. [ntl.bts.gov/lib/46000/46200/46247/SPR\\_688.pdf](http://ntl.bts.gov/lib/46000/46200/46247/SPR_688.pdf).
- Karamihas, S. M. and K. Senn. 2012. *Curl and Warp Analysis of the LTPP SPS-2 Site in Arizona*. Report FHWA-HRT-12-068. Federal Highway Administration, McLean, VA.
- Kim, S., K. Gopalakrishnan, H. Ceylan, and K. Wang. 2010. Early-age response of concrete pavements to temperature and moisture variations. *The Baltic Journal of Road and Bridge Engineering*. 5 (3): 132–138.

- Lederle, R. E., R. W. Lothschutz, and J. E. Hiller. 2011. *Field Evaluation of Built-In Curling Levels in Rigid Pavements*. Minnesota Department of Transportation, St. Paul, MN.
- Lim, J., A. Azary, L. Khazanovich, S. Wang, S. Kim, H. Ceylan, and K. Gopalakrishnan. 2012. *Effects of Implements of Husbandry (Farm Equipment) on Pavement Performance*. Report MN/RC 2012-08. Minnesota Department of Transportation, St. Paul, MN.
- Macro Sensors. 2014. *LVDT Basics*. Technical Bulletin. Pennsauken, NJ.  
[www.macrosensors.com/lvdt\\_tutorial.html](http://www.macrosensors.com/lvdt_tutorial.html). Last accessed January 4, 2016.
- Mailvaganam, N., J. Springfield, W. Repette, and D. Taylor. 2000. *Curling of Concrete Slabs on Grade*. Institute for Research in Construction, National Research Council of Canada,  
[www.nrc-cnrc.gc.ca/ctu-sc/files/doc/ctu-sc/ctu-n44\\_eng.pdf](http://www.nrc-cnrc.gc.ca/ctu-sc/files/doc/ctu-sc/ctu-n44_eng.pdf). Last accessed December 30, 2015.
- MATEST. No date. *B099KIT MOT Straight Edge*, [www.matest.com/en/Products/bitumen-asphalt/Macro-Category/OTHER%20PRODUCTS-1-1-1/b099kit-mot-straight-edge](http://www.matest.com/en/Products/bitumen-asphalt/Macro-Category/OTHER%20PRODUCTS-1-1-1/b099kit-mot-straight-edge). Last accessed January 4, 2016.
- Mike Petsch & Associates, Inc. no date. *Precision Straight Edges for Checking Airport Pavement Smoothness*. Mike Petsch & Associates, Inc., Dayton, OH.  
[petsch.cnc.net/web/Runway/RunwayStraighEdge.htm](http://petsch.cnc.net/web/Runway/RunwayStraighEdge.htm).
- MnDOT. 2009. Rutting-ALPS. *MnROAD*. Minnesota Department of Transportation, Monticello, MN. [www.dot.state.mn.us/mnroad/data/pdfs/alps.pdf](http://www.dot.state.mn.us/mnroad/data/pdfs/alps.pdf). Last accessed December 30, 2015.
- . 2011. HMA Rutting. *MnROAD*. Minnesota Department of Transportation, Monticello, MN.
- Morrow, G. 2006. Comparison of roughness measuring instruments. Thesis, University of Auckland.
- Nantung, T. E. 2011. *High Performance Concrete Pavement in Indiana*. Report FHWA/IN/JTRP-2011/20. Division of Research and Development, Indiana Department of Transportation, West Lafayette, IN.
- Nassiri, S. 2011. Establishing permanent curl/warp temperature gradient in jointed plain concrete pavements. PhD dissertation, University of Pittsburgh.
- Olson, M. J. and A. Chin. 2012. *Inertial and Inclinomater Based Profiler Repeatability and Accuracy Using the IRI Model*. Report SPR 744. Oregon Department of Transportation Research Section and Federal Highway Administration.
- Pavement Interactive. 2007. Pavement Management: Roughness. *Pavement Interactive*.  
[www.pavementinteractive.org/article/roughness/](http://www.pavementinteractive.org/article/roughness/). Last accessed January 4, 2016.
- Pavement Interactive. 2010. The Smoothness Playbook, *Pavement Interactive*.  
[www.pavementinteractive.org/2010/08/24/the-smoothness-playbook/](http://www.pavementinteractive.org/2010/08/24/the-smoothness-playbook/). Last accessed January 4, 2016.
- Perera, R. W. and S. D. Kohn. 2005. *Quantification of Smoothness Index Differences Related to Long-Term Pavement Performance Equipment Type*. Report FHWA-HRT-05-054. Federal Highway Administration, McLean, VA.
- Perera, R. W., S. D. Kohn, and G. R. Rada. 2002. *LTPP Manual for Profile Measurements Operational Field Guidelines Version 4.0*. Report DTFH61-02-C-00007. Federal Highway Administration, McLean, VA.
- Perera, R. W., S. D. Kohn, and S. Tayabji. 2005. *Achieving a High Level of Smoothness in Concrete Pavements without Sacrificing Long-Term Performance*. Report FHWA-HRT-05-069. Federal Highway Administration, McLean, VA.

- Rao, S. and J. R. Roesler. 2005. Characterizing effective built in curling from concrete pavement field measurements. *Journal of Transportation Engineering, ASCE* 131 (4): 320–327.
- Sayers, M. W. and S. M. Karamihas. 1998. *The Little Book of Profiling*. The Regent of the University of Michigan.
- Schwartz, C. W., R. Li, S. Kim, H. Ceylan, and K. Gopalakrishnan. 2011. *Sensitivity Evaluation of MEPDG Performance Prediction*. Contractor's Final Report of NCHRP 1-47 project. University of Maryland and Iowa State University.
- Smith, K. L., L. Titus-Glover, and L. D. Evans. 2002. *Pavement Smoothness Index Relationships*. Report FHWA-RD-02-057. Office of Pavement Technology, Federal Highway Administration, Washington, DC.
- Suprenant, B. A. and W. R. Malisch. 1999. Repairing curled slabs. *Concrete Construction* 9:58–65.
- Teller, L. W. and E. C. Sutherland. 1935. The structural design of concrete pavements, part 2: Observed effects of variations in temperature and moisture on the size, shape, and stress resistance of concrete pavement slabs. *Public Roads* 16 (9): 169–197.
- Transtec Group, Inc. 2012. Understanding Smoothness Specifications. *SmoothPavements*. Austin, TX. [www.smoothpavements.com/content.aspx?id=1](http://www.smoothpavements.com/content.aspx?id=1). Last accessed December 30, 2015.
- Trimble. 2015. *Spectra Precision® DR400 DigiRod*, [www.trimble.com/construction-tools/dr400.aspx?dtID=overview&](http://www.trimble.com/construction-tools/dr400.aspx?dtID=overview&). Last accessed December 30, 2015.
- Tsai, Y. C. J. and F. Li. 2012. Critical assessment of detecting asphalt pavement cracks under different lighting and low intensity contrast conditions using emerging 3D laser technology. *Journal of Transportation Engineering, ASCE* 138 (5): 649–656.
- University of Utah Civil Engineering Students Creative Commons. 2011. CVEEN 7570- Spring 2011. *PaveMaintenance*. [pavemaintenance.wikispaces.com/CVEEN+7570+Spring+2011](http://pavemaintenance.wikispaces.com/CVEEN+7570+Spring+2011). Last accessed January 4, 2016.
- Van Dam, T. 2015. *Concrete Pavement Curling and Warping: Observations and Mitigation*. MAP Brief April 2015, [www.cproadmap.org/publications/MAPbriefApril2015.pdf](http://www.cproadmap.org/publications/MAPbriefApril2015.pdf). Last accessed December 30, 2015.
- Wells, S. A. 2005. Early age response of jointed plain concrete pavements to environmental loads. Thesis, University of Pittsburgh.
- Worel, B., B. Chadbourn, and R. Strommen. 2004. MnROAD Automated Laser Profile System (ALPS). Paper presented at the 2nd International Conference on Accelerated Pavement Testing, Minneapolis, MN, September 26-29, 2004.
- Wright-Kehner, E. 2015. *Research Section*. Arkansas State Highway and Transportation Department. [www.arkansashighways.com/System\\_Info\\_and\\_Research/research.aspx](http://www.arkansashighways.com/System_Info_and_Research/research.aspx). Last accessed January 4, 2016.



## **APPENDIX A. FOURTH-GENERATION ISU CURLING AND WARPING MEASUREMENT DEVICE**



**Figure A.1. Side view of ISU curling and warping measurement device**

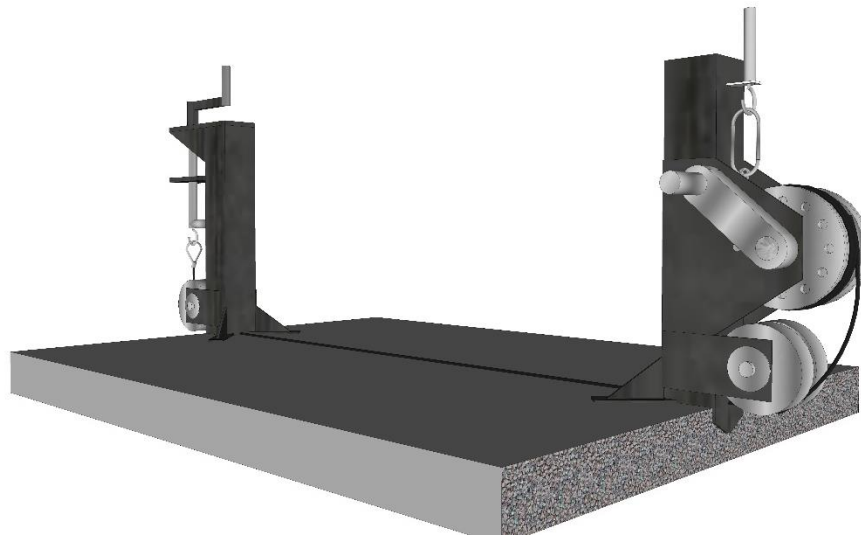


**Figure A.2. 3D view of device from column A**

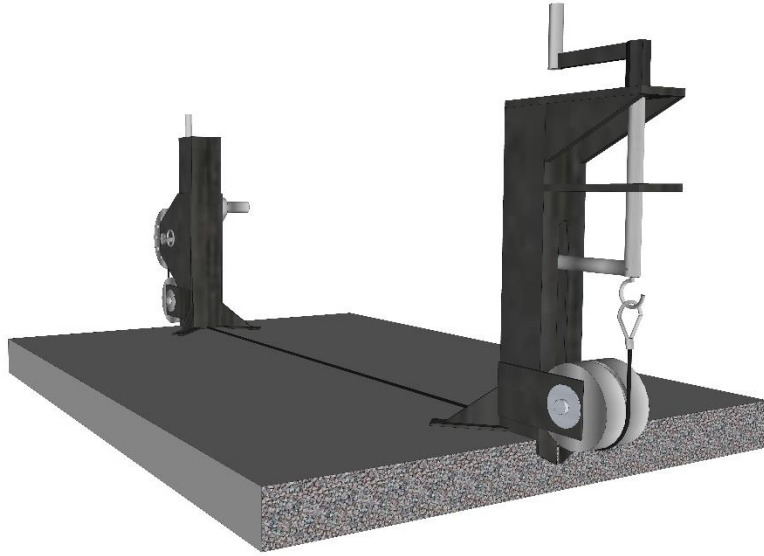


**Figure A.3. 3D view of device from column B**

## APPENDIX B. FOURTH-GENERATION ISU CURLING AND WARPING MEASUREMENT DEVICE SCHEMATIC



Figure B.1. Dimension diagram of ISU curling and warping measurement device





## **APPENDIX C. ISU CURLING AND WARPING MEASUREMENT DEVICE OPERATION MANUAL**

1. Place the main parts of the ISU curling and warping measurement device (e.g., columns A and B, measuring gauge, and digital height gauge), accessories (measuring tape, iron bricks, clips, and pins), and other materials (trowel, small knife, and infrared temperature gun) into a bucket and transport them to the predetermined PCC slab.
2. Determine the start point at the joint and then insert the anchor of column A into the joint. The trowel and small knife can be used to cut a small gap on the joint sealant (Figure C.1).

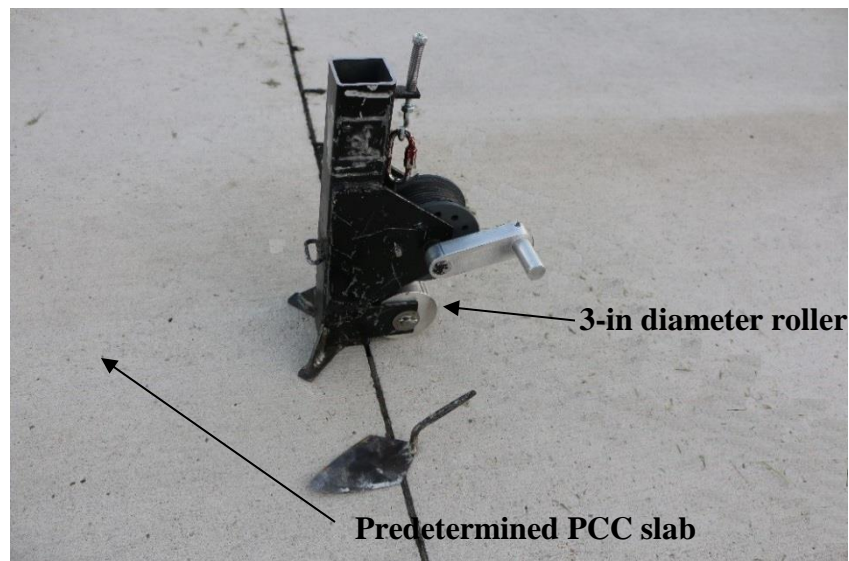


**Figure C.1. Insert anchor of column A into the joint**

3. Unpin the sliver steel bar from the U-groove wheel and unhook the string from column A (Figure C.2).

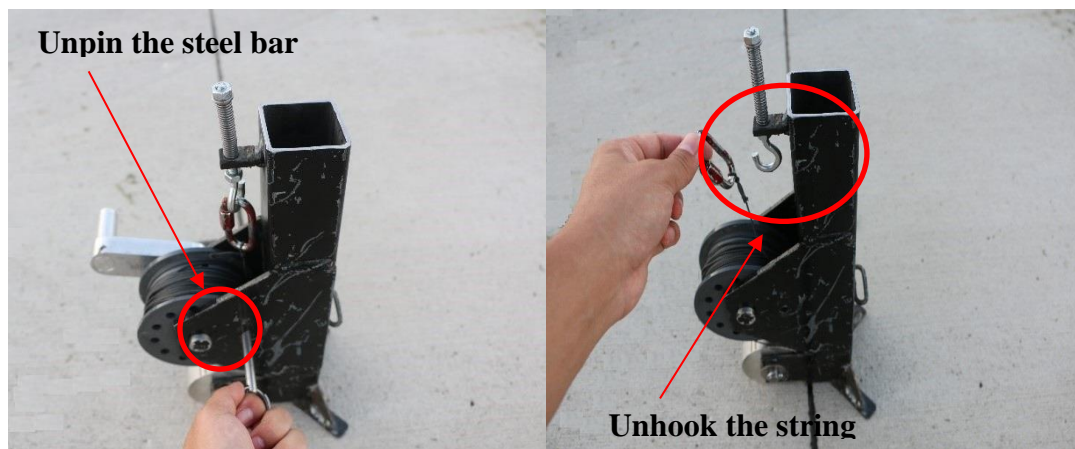


**Figure C.2. Unpin the bar and unhook the string**

4. Drag the string to pass through column A from the bottom of 3-in diameter roller and the empty space in the middle of anchor (Figure C.3).

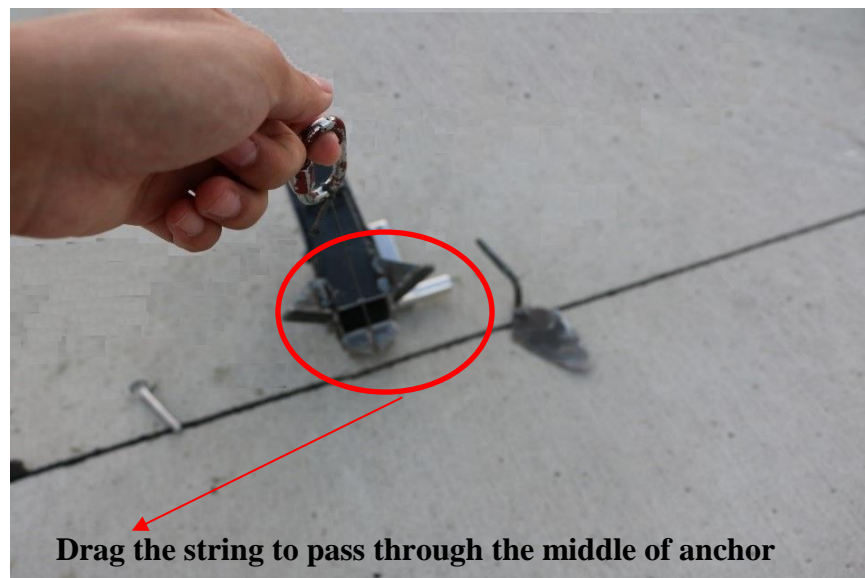


**Figure C.3. Pull the string out**

5. Repeat the same procedures on the opposite joint and insert column B.
6. Draw the string to the 3-inch-diameter roller in column B and hook it up at the bottom of the bolt (make sure the string is in the small groove on the roller) (Figure C.4).

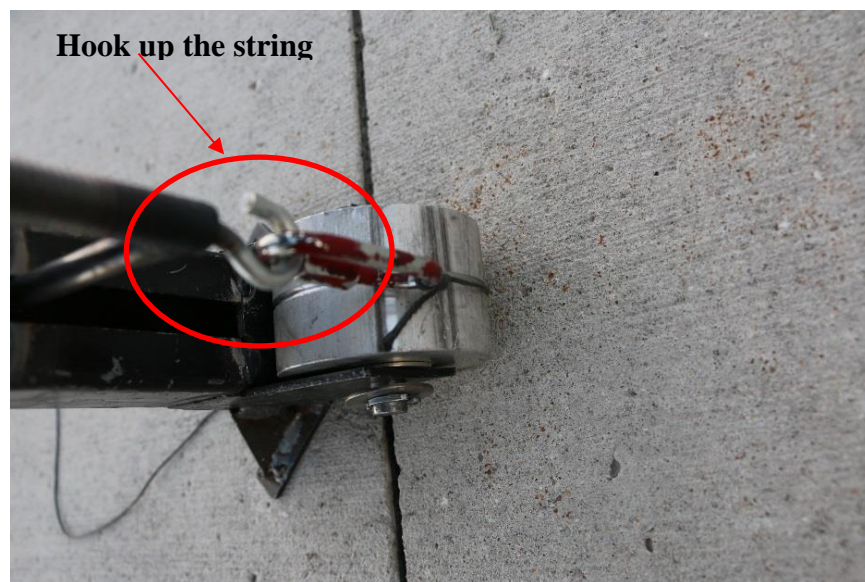


**Figure C.4. Hook up the string in column B**

7. Adjust the crank of column A to make the string tight and then insert the small sliver steel bar into the holes to lock the U-groove wheel when the hole in the flange and the hole in the welded metal plate are in the small line (Figure C.5).

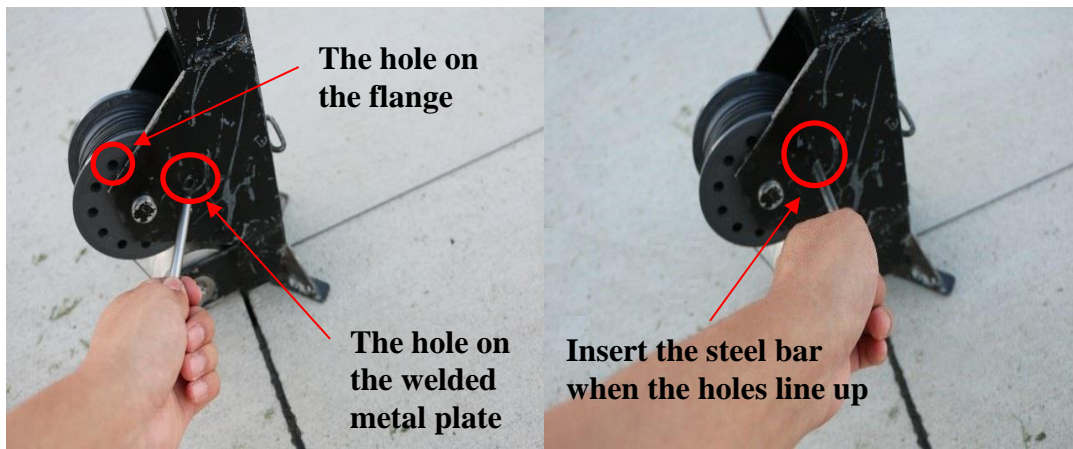


**Figure C.5. Lock the U-groove wheel in column A**

8. Place the red pins under the string close to the columns and then rotate the handle of column B to move the bolt up to further tighten the string (but do not overtighten) (Figure C.6).

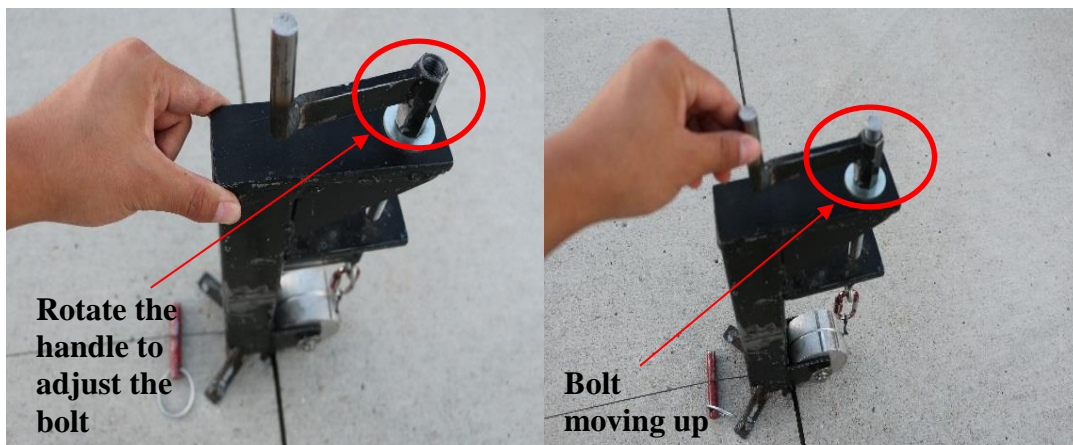


**Figure C.6. Adjust the handle of column B to further tighten the string**

9. Insert clips at the bottom of columns (Figure C.7).





**Figure C.7. Insert the clips**

10. Deploy the measuring tape beside the string and use iron bricks to restrain any movement caused by wind (Figure C.8).

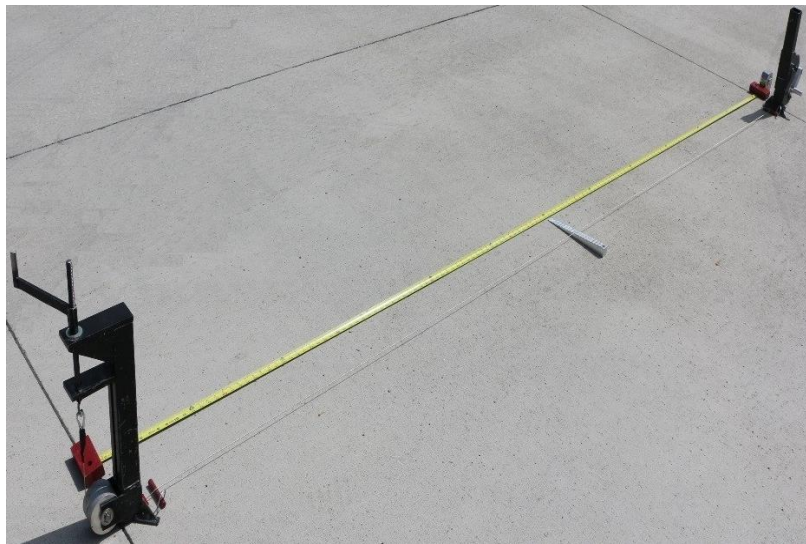


**Figure C.8. Deploy the measuring tape**

11. Use the measuring gauge or digital height gauge to measure the deflection at the predetermined point along the string (Figure C.9).



**Figure C.9. Take measurements using rulers**

12. Record data.